ROYAL INSTITUTE
OF TECHNOLOGY

Response Matrix Reloaded

For Monte Carlo Simulations in Reactor Physics

IGNAS MICKUS

Licentiate Thesis
Stockholm, Sweden 2019

AlbaNova
Roslagstullsbacken 21
SE-10691 Stockholm
Sweden

TRITA-SCI-FOU 2019:54
ISBN 978-91-7873-384-2

Akademisk avhandling som med tillstånd av Kungl Tekniska högskolan framlägges till offentlig granskning för avläggande av teknologie licentiatexamen i kärnenergiteknik tisdagen den 10 december 2019 klockan 14.00 i FB54, AlbaNova Universitetscentrum, Roslagstullsbacken 21, Stockholm.

Tryck: Universitetsservice US AB

Abstract

This thesis investigates Monte Carlo methods applied to criticality and time-dependent problems in reactor physics. Due to their accuracy and flexibility, Monte Carlo methods are considered as a "gold standard" in reactor physics calculations. However, the benefits come at a significant computing cost. Despite the continuous rise in easily accessible computing power, a brute-force Monte Carlo calculation of some problems is still beyond the reach of routine reactor physics analyses. The two papers on which this thesis is based try to address the computing cost issue, by proposing methods for performing Monte Carlo reactor physics calculations more efficiently. The first method addresses the efficiency of the widely-used k-eigenvalue Monte Carlo criticality calculations. It suggests, that the calculation efficiency can be increased through a gradual increase of the neutron population size simulated during each criticality cycle, and proposes a way to determine the optimal neutron population size. The second method addresses the application of Monte Carlo calculations to reactor transient problems. While reactor transient calculations can, in principle, be performed using only Monte Carlo methods, such calculations take multiple thousands of CPU hours for calculating several seconds of a transient. The proposed method offers a middle-ground approach, using a hybrid stochastic-deterministic scheme based on the response matrix formalism. Previously, the response matrix formalism was mainly considered for steady-state problems, with limited application to time-dependent problems. This thesis proposes a novel way of using information from Monte Carlo criticality calculations for solving time-dependent problems via the response matrix.

Sammanfattning

Denna avhandling undersöker Monte Carlo-metoder som används för kritikalitets- och tidsberoende problem i reaktorfysik. På grund av deras noggrannhet och flexibilitet betraktas Monte Carlo-metoder som en 'gyllene standard' i reaktorfysikberäkningar. Fördelarna kommer dock till priset av betydande datorkostnad. Trots den kontinuerliga ökningen av lättillgänglig datorkraft är en råstyrka Monte Carlo-beräkningar av vissa problem fortfarande utanför räckvidden för reaktorfysikaliska rutinanalyser. De två artiklarna som denna avhandling bygger på försöker ta itu med beräkningskostnadsproblemet genom att föreslå metoder för att utföra Monte Carlo-reaktorfysikberäkningar mer effektivt. Den första metoden behandlar effektiviteten för de vitt använda beräkningarna av k-egenvärdet med Monte Carlo. Den antyder att beräkningseffektiviteten kan ökas genom en gradvis ökning av neutronpopulationens storlek som simuleras under varje kritikalitetscykel, och föreslår ett sätt att bestämma den optimala neutronpopulationens storlek. Den andra metoden behandlar tillämpningen av Monte Carlo-beräkningar för reaktortransienter. Medan beräkningar av reaktortransienter i princip kan utföras uteslutande med Monte Carlo-metoder, tar sådana beräkningar flera tusentals CPU-timmar för att beräkna flera sekunder av en transient. Den föreslagna metoden erbjuder en medelväg, med användning av ett stokastiskt-deterministiskt hybridschema baserat på responsmatrisformalismen. Tidigare har responsmatrisformalismen huvudsakligen beaktats för tidsoberoende problem, med begränsad tillämpning på tidsberoende problem. Denna avhandling föreslår ett nytt sätt att använda information från Monte Carlo-kritikalitetsberäkningar för att lösa tidsberoende problem via responsmatrisen.

List of Papers

Included Papers

The thesis is based on the following papers:

I I. Mickus and J. Dufek, "Optimal neutron population growth in accelerated Monte Carlo criticality calculations," *Annals of Nuclear Energy* vol. 117, pp. 297-304, 2018.

II I. Mickus, J. A. Roberts, and J. Dufek, "Stochastic-deterministic response matrix method for reactor transients," *Annals of Nuclear Energy*, in press, 2019.

Author's Contribution

The author has devised the method in Paper I together with J. Dufek, performed all calculations and wrote the text. The author has devised the method in Paper II, performed all calculations and wrote the text in collaboration with J. A. Roberts.

Papers not Included that Relate to the Thesis Topic

1. J. Dufek and I. Mickus, "Optimal time step length and statistics in Monte Carlo burnup simulations," *Annals of Nuclear Energy*, submitted for publication, 2019.

2. I. Mickus, J. Dufek, and K. Tuttelberg, "Performance of the explicit Euler and predictor-corrector-based coupling schemes in Monte Carlo burnup calculations of fast reactors," *Nuclear Technology*, vol. 191, no. 2, pp. 193-198, 2015.

3. I. Mickus, J. Dufek, and K. Tuttelberg, "Comparative study of the explicit Euler and predictor-corrector based coupling schemes in Monte Carlo burnup calculations of fast and thermal reactors," in *The 17th meeting on Reactor Physics in the Nordic Countries*, (Gothenburg, Sweden), 2015.

Other Publications

1. C. Geffray, A. Gerschenfeld, P. Kudinov, I. Mickus, M. Jeltsov, K. Kööp, D. Grishchenko, and D. Pointer, "Verification and validation and uncertainty quantification," in *Thermal Hydraulics Aspects of Liquid Metal Cooled Nuclear Reactors* (F. Roelofs, ed.), ch. 8, pp. 383-405, Woodhead Publishing, 2019.

2. J. Wallenius, S. Qvist, I. Mickus, S. Bortot, P. Szakalos, and J. Ejenstam, "Design of SEALER, a very small lead-cooled reactor for commercial power production in off-grid applications," *Nuclear Engineering and Design*, vol. 338, pp. 23-33, 2018.

3. J. Wallenius, S. Bortot, and I. Mickus, "Unprotected transients in SEALER: A small lead-cooled reactor for commercial power production in Arctic regions," in *PHYSOR 2018: Reactors Physics paving the way towards more efficient systems*, (Cancun, Mexico), 2018.

4. I. Mickus, J. Wallenius, and S. Bortot, "Preliminary Transient Analysis of SEALER," in *Fast Reactors and Related Fuel Cycles: Next Generation Nuclear Systems for Sustainable Development (FR17)*, (Jekaterinburg, Russian Federation), 2017.

5. J. Wallenius, S. Qvist, I. Mickus, S. Bortot, J. Ejenstam, and P. Szakalos. "SEALER: A small lead-cooled reactor for power production in the Canadian Arctic," in *Fast Reactors and Related Fuel Cycles: Next Generation Nuclear Systems for Sustainable Development (FR17)*, (Jekaterinburg, Russian Federation), 2017.

6. S. Bortot, I. Mickus, and J. Wallenius, "Preliminary Safety Performance Assessment of ESFR CONF-2 Sphere-Pac-Fueled Core," in *Fast Reactors and Related Fuel Cycles: Next Generation Nuclear Systems for Sustainable Development (FR17)*, (Jekaterinburg, Russian Federation), 2017.

7. P. Larroche, S. Bortot, J. Wallenius, and I. Mickus, "Design of a Nitride-fuelled Lead Fast Reactor for Minor Actinides Transmutation," in *Fast Reactors and Related Fuel Cycles: Next Generation Nuclear Systems for Sustainable Development (FR17)*, (Jekaterinburg, Russian Federation), 2017.

8. D. Grishchenko, K. Kööp, M. Jeltsov, I. Mickus, and P. Kudinov "TALL-3D test series for calibration and validation of coupled thermal-hydraulics codes," in *17th International Topical Meeting on Nuclear Reactor Thermal Hydraulics (NURETH-17)*, (Xian, China), 2017.

9. I. Mickus, K. Kööp, M. Jeltsov, D. Grishchenko, P. Kudinov, J. Lappalainen, "Development of TALL-3D Test Matrix for APROS Code Validation," in *16th International Topical Meeting on Nuclear Reactor Thermalhydraulics (NURETH-16)*, (Chicago, USA), 2015.

10. I. Mickus, J. Lappalainen, P. Kudinov, "Validation of APROS code against experimental data from a lead-bismuth eutectic thermal-hydraulic loop," in *2015 International Congress on Advances in Nuclear Power Plants (ICAPP '15)*, (Nice, France), 2015.

11. I. Mickus, K. Kööp, M. Jeltsov, Y. Vorobyev, W. Villanueva, P. Kudinov, "An Approach to Physics Based Surrogate Model Development for Application with IDPSA," in *Probabilistic Safety Assessment and Management (PSAM 12)*, (Honolulu, Hawaii), 2014.

Acknowledgements

I would like to thank my supervisor dr. Jan Dufek for providing me with the opportunity to work on this topic and advising me throughout the process. I am grateful to dr. Jeremy A. Roberts for the fruitful and motivating discussions we had on the response matrix methods. Furthermore, my regards to the colleagues in the Nuclear Engineering division for your help, lunch conversations, and the pleasant working environment. Finally, to my friends and family, thank you for your continuous support and encouragement.

The author performed the work supported by the McSAFE project which is receiving funding from the Euratom research and training programme 2014-2018 under grant agreement No 755097.

Calculations presented in Paper I were performed on resources provided by the Swedish National Infrastructure for Computing (SNIC) at PDC Centre for High Performance Computing (PDC-HPC).

Contents

Thank you industrialization. Thank you steel mill. Thank you power station. And thank you chemical processing industry that gave us time to read books.

Hans Rosling (1948-2017)

Chapter 1

Introduction

1.1 Background

Achieving the climate goals given the projected increase in global energy demand will require the deployment of sustainable energy generation technologies. According to the report by the United Nations Intergovernmental Panel on Climate Change [1], the share of nuclear power in the primary energy supply should increase in most scenarios with no or limited overshoot of the 1.5 °C global warming target by the year 2050. However, the projected share varies significantly between the different scenarios, ranging from an increase of more than 700 % to a decrease of 36 % in several scenarios. Such a large variation is attributed to the fact that the future deployment of nuclear power can be constrained by societal preferences. To help address the societal concerns, robust analyses of design, deployment, operation and decommissioning of nuclear systems are required. Hence, future deployment of nuclear power is subject to the availability of accurate and efficient methods to support the analyses.

Most of the existing computational tools in reactor physics analyses are based on deterministic methods that solve the neutron transport equation. To obtain a numerical solution, this equation needs to be severely simplified, introducing assumptions to the analyses and taking into account the peculiarities of the modelled systems. Consequently, deterministic methods become tailored to a specific reactor design. Every modification made to the design, or the assumptions applied in the analyses, then requires cumbersome altering of computing routines and nuclear data libraries. Monte Carlo methods are not tailored to a specific reactor design since these methods simulate the actual collisions of billions of neutrons in any geometry. Therefore, Monte Carlo methods, due to their versatility and lack of approximations to neutron transport, are widely applied to research and development of existing and new nuclear systems.

Computational tools based on Monte Carlo methods are flexible, accurate, but bare a high computing cost. Because of the stochastic nature, Monte Carlo methods

require a significant computing effort to reduce the statistical error to an acceptable degree. The increase of available computing power in recent decades enabled the application of Monte Carlo methods to a wider range of reactor physics problems. Still, Monte Carlo simulations of some large-scale problems are considered computationally too expensive for routine analyses. Consequently, ways to use the Monte Carlo methods more efficiently need to be developed.

1.2 Scope and Objective

This thesis focuses on two areas of Monte Carlo calculations in reactor physics: Monte Carlo criticality calculations and Monte Carlo methods for reactor kinetics calculations. The methods proposed in the included papers aim at improving the efficiency of these calculations.

1.3 Thesis Structure

The thesis is structured as a compilation thesis. Correspondingly, the author's main contribution is presented in the included papers, while Chapters 2 and 3 are intended to provide introductory information supporting the included papers. Chapter 2 provides an introduction to neutron transport, Monte Carlo methods in reactor physics, and discusses some aspects of the Monte Carlo fission source convergence, together with a summary of the previous work on the topic. Chapter 3 discusses the application of Monte Carlo methods for solving time-dependent reactor physics problems. It provides an overview of the time-dependent Monte Carlo method together with several hybrid stochastic-deterministic schemes previously proposed for time-dependent problems. The included papers are summarized in Chapter 4. Finally, conclusions for this thesis together with an outlook for the future work are given in Chapter 5.

Chapter 2

Criticality Problems

This chapter is intended to provide the background material supporting Paper I. It starts with a general discussion on neutron transport and the k-eigenvalue formulation of the neutron transport equation. Even though this formalism is not required for understanding the Monte Carlo procedure in reactor physics calculations, it is instructive for interpreting the features of Monte Carlo calculations. The chapter then continues with the discussion of fission source convergence, and finally overviews the fission matrix, the response matrix and the neutron population size optimization techniques proposed for improving the efficiency of Monte Carlo criticality calculations.

2.1 Neutron Transport

One of the central problems in reactor physics is to determine the space, energy and time distribution of neutrons in a specific geometry, such as the core of a nuclear reactor [2]. Other quantities of interest can be derived from this distribution. The behaviour of neutrons is described by the neutron transport theory, which characterizes the motion of neutrons undergoing multiple scattering events until eventually being absorbed, or leaking out of the system.

To describe neutron transport, we need to define several quantities which adequately describe the state of a neutron for reactor analyses. Fist, we need to introduce the concept of *angular neutron density*, n [3]:

$$n(\mathbf{r}, \mathbf{\Omega}, E, t)\mathrm{d}\mathbf{r}\mathrm{d}\mathbf{\Omega}\mathrm{d}E, \tag{2.1}$$

which gives the expected number of neutrons in a volume d$\mathbf{r}$ about $\mathbf{r}$, moving in direction $\mathbf{\Omega}$ in solid angle d$\mathbf{\Omega}$, with energies dE about E at time t. Hence, neutrons as described by the transport theory exist in a seven-dimensional phase-space ($\mathbf{r} = x, y, z; \mathbf{\Omega} = \theta, \varphi; E; t$). Notice, that the definition includes the term *expected*, which means that the transport theory is defined for the average behaviour

of the neutron population, while the quantities associated with the real population would fluctuate around the expected values.

A related concept is the *angular neutron flux*, ψ, which is obtained by multiplying the angular density by the neutron speed (the absolute value of velocity vector), v [3]:

$$\psi(\mathbf{r}, \mathbf{\Omega}, E, t) \equiv vn(\mathbf{r}, \mathbf{\Omega}, E, t). \tag{2.2}$$

The angular neutron flux is simply a mathematical definition used in place of the product $vn(\mathbf{r}, \mathbf{\Omega}, E, t)$ for convenience when expressing reaction rate densities

$$f(\mathbf{r}, \mathbf{\Omega}, E, t) = v\Sigma(\mathbf{r}, E)n(\mathbf{r}, \mathbf{\Omega}, E, t) = \Sigma(\mathbf{r}, E)\psi(\mathbf{r}, \mathbf{\Omega}, E, t), \tag{2.3}$$

where Σ is used to denote the macroscopic cross-section. Definitions of other related concepts, such as the angular current density $\mathbf{j}(\mathbf{r}, \mathbf{\Omega}, E, t)$, and the corresponding scalar quantities are omitted from this description for the sake of brevity[1].

The neutron transport theory further consides balances of various mechanisms by which neutrons can be gained or lost from an arbitrary phase-space element. This results in the time-dependent neutron transport equation [3]

$$\begin{aligned} &\frac{1}{v}\frac{\partial}{\partial t}\psi(\mathbf{r}, \mathbf{\Omega}, E, t) + \mathbf{\Omega} \cdot \nabla\psi(\mathbf{r}, \mathbf{\Omega}, E, t) + \Sigma_t(\mathbf{r}, E)\psi(\mathbf{r}, \mathbf{\Omega}, E, t) = \\ q_{ex}(\mathbf{r}, \mathbf{\Omega}, E, t) &+ \int_{4\pi} \mathrm{d}\mathbf{\Omega}' \int_0^\infty \mathrm{d}E' \Sigma_s(\mathbf{r}, \mathbf{\Omega}' \to \mathbf{\Omega}, E' \to E)\psi(\mathbf{r}, \mathbf{\Omega}', E', t) + \\ &\frac{\chi(\mathbf{r}, E)}{4\pi} \int_{4\pi} \mathrm{d}\mathbf{\Omega}' \int_0^\infty \mathrm{d}E' \nu(\mathbf{r}, E')\Sigma_f(\mathbf{r}, E')\psi(\mathbf{r}, \mathbf{\Omega}', E', t), \end{aligned} \tag{2.4}$$

where $\Sigma_t(\mathbf{r}, E)$, $\Sigma_s(\mathbf{r}, E')$ and $\Sigma_f(\mathbf{r}, E')$ denote the macroscopic total, scattering and fission cross-sections respectively, $\chi(\mathbf{r}, E)$ gives the fission neutron energy distribution, and $\nu(\mathbf{r}, E')$ denotes the average number of neutrons emitted in a fission reaction induced by a neutron with energy E'. In general, these parameters depend on time, which was suppressed here. The first term on the right-hand side of Eq. (2.4) describes the change of angular neutron density in time, the second term describes streaming, the third term describes all interactions which yield neutron removal from the flux (scattering out from the phase-space element and absorption). The left-hand side terms describe sources; here the first term describes neutrons added to the flux by external sources, the second and third terms describe neutrons added to the flux due to scattering into the phase-space element and due to fission respectively. Note, that in Eq. (2.4) all neutrons are assumed to appear instantaneously at the time of fission. The concept of delayed neutrons, which is important in solving time-dependent reactor physics problems, will be introduced in Chapter 3, together with the necessary modifications to Eq. (2.4).

Owing to complex dependencies of parameters, such as continuous variation of reaction cross-sections with neutron energy, angular dependencies, the geometrical arrangement of materials in a nuclear reactor, and the general form of the

[1] A detailed description can be found in any textbook on nuclear reactor theory, e.g. [2,3]

Eq. (2.4), a direct analytical solution is possible only for several highly simplified problems. A direct numerical solution of the neutron transport equation is computationally prohibitive. Therefore various approximate forms are used to formulate the deterministic solution methods. The approximations include various schemes for discretization in space, time, energy and angle, application of diffusion theory or point-kinetics models, flux factorisation, and other [4].

2.2 Monte Carlo Simulation of Neutron Transport

The neutron transport equation is useful for explaining the physical concepts and is a starting point for deriving various deterministic methods. However, the transport equation is not necessary for solving a problem using Monte Carlo methods. This leads to one of the common misconceptions in Monte Carlo particle transport — that Monte Carlo methods solve the transport equation [7]. Monte Carlo methods theoretically duplicate (simulate) the stochastic transport of individual particles in a system and infer the average behaviour of particles in a real system from the average behaviour of the simulated particles [8]. The transport equation, on the other hand, describes the average particle behaviour by definition, as indicated in Section 2.1. Monte Carlo simulation yields the same mean result as the original problem, i.e. the average neutron behaviour in a Monte Carlo simulation is described by the neutron transport equation.

Monte Carlo particle transport simulation is conducted by sequentially following the probabilistic events that constitute histories of individual particles. The events constituting a history are statistically sampled from probability distributions characterizing the physical phenomena, using random numbers. The characteristics of the system are then inferred from simulating a large number of particle histories.

Figure 2.1 illustrates a Monte Carlo reactor physics simulation. Monte Carlo reactor physics codes simulate the histories of individual neutrons[2] by following the neutron's interaction with matter in a specific geometry, starting from a source until eventual absorption or leakage out of the system. Quantities of interest are scored (tallied) during the simulation, together with statistical precision estimates.

Following the history of each neutron by explicitly simulating every event (e.g. scattering, fission, capture, etc.) would yield an *analog* Monte Carlo simulation. The statistical variance of such simulation would correspond to the natural variance of the simulated process. This means that a very large number of histories would need to be simulated to collect results with acceptable statistical precision, especially if the events with a low probability of occurrence are of interest. Hence, for many reactor physics applications, the analog approach would lead to unacceptable computing time requirements. This problem is resolved by applying various *non-analog* Monte Carlo methods. These methods, called variance reduction techniques, bias the analog transport process in a way that the events of interest occur

[2]Some reactor physics codes have capabilities for coupled neutron-photon transport simulations [8, 9]. Monte Carlo photon transport is beyond the scope of this thesis.

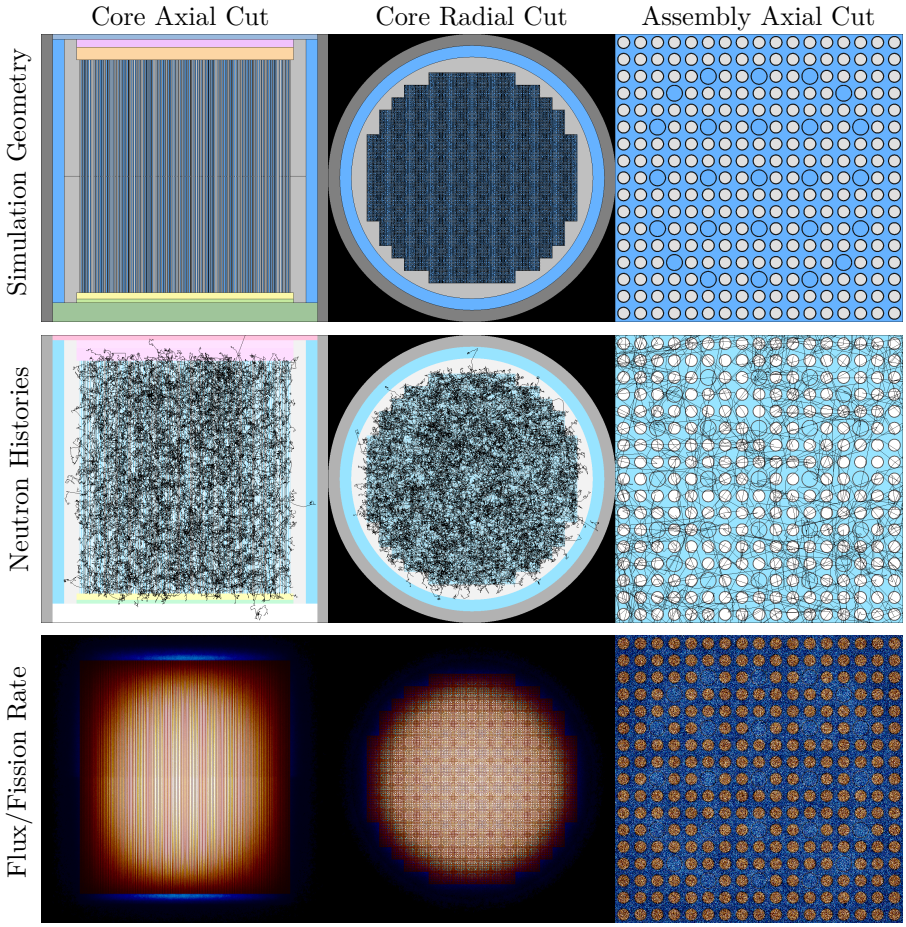

Figure 2.1: Illustration of a Monte Carlo reactor physics simulation. The images were generated with the Serpent 2 Monte Carlo reactor physics code [5] using the PWR performance benchmark geometry [6].

more frequently. To assure that the results are not biassed (i.e. the expected value of a non-analog simulation is equal to that of the analog simulation), each neutron is assigned a statistical weight which is modified every time the analog transport process is changed. The results are then scored considering the statistical weight of each neutron contributing to a specific result.

Monte Carlo calculations in reactor physics can be classified into three broad categories based on problem formulation: fix source calculations, criticality calculations, and transient calculations. Fixed source calculations follow neutron histories

from a user-defined source through a multiplying or a non-multiplying medium. If the medium is multiplying, the histories are not terminated at fission events, but rather split into two or more new paths [10]. A steady-state solution for such problem exists only if the multiplying medium is sub-critical. Fixed source calculations are used in, among other, shielding problems, dose rate calculations, or analysis of sub-critical accelerator-driven systems. Criticality calculations are discussed in the following section, while transient calculations are discussed in Chapter 3.

2.3 Monte Carlo Criticality Calculations

Most Monte Carlo codes that perform criticality calculations simulate the steady-state k-eigenvalue problem[3]. The k-eigenvalue problem can be understood by examining several concepts following from the neutron transport equation. The neutron transport equation seeks for a time-dependent solution for a given initial neutron population. Indeed, a non-zero initial neutron population will die out in a sub-critical multiplying system unless maintained by an external neutron source or diverge in a super-critical multiplying system. A steady-state (time-independent) neutron population is possible either in a sub-critical system with an external neutron source, or if the system is *exactly* critical.

However, such *exactly* critical systems are practically not attainable neither in reality nor in a numerical model. Real systems are continuously balanced between slightly sub-critical and slightly super-critical states by e.g. movement of control rods. A common way of dealing with this problem in numerical models is to scale the value of $\nu(\mathbf{r}, E')$ by a factor k such that the solution becomes time-independent. Then, dropping the time derivative term and setting the external source q_{ext} to zero in Eq. (2.4) yields

$$\begin{aligned} \boldsymbol{\Omega} \cdot \nabla\psi(\mathbf{r}, \boldsymbol{\Omega}, E) + \Sigma_t(\mathbf{r}, E)\psi(\mathbf{r}, \boldsymbol{\Omega}, E) = \\ \int_{4\pi} \mathrm{d}\boldsymbol{\Omega}' \int_0^\infty \mathrm{d}E' \Sigma_s(\mathbf{r}, \boldsymbol{\Omega}' \to \boldsymbol{\Omega}, E' \to E)\psi(\mathbf{r}, \boldsymbol{\Omega}', E') + \\ \frac{1}{k}\frac{\chi(\mathbf{r}, E)}{4\pi} \int_{4\pi} \mathrm{d}\boldsymbol{\Omega}' \int_0^\infty \mathrm{d}E' \nu(\mathbf{r}, E')\Sigma_f(\mathbf{r}, E')\psi(\mathbf{r}, \boldsymbol{\Omega}', E'). \end{aligned} \tag{2.5}$$

This modification turns Eq. (2.4) into an eigenvalue equation which has k_i eigenvalues together with the associated eigenfunctions ψ_i, where the largest eigenvalue k_0 has a physical meaning as the effective multiplication factor $k_0 = k_{eff}$, and the associated eigenfunction ψ_0 gives the fundamental mode for the distribution of neutrons in the system. Systems with $k_{eff} > 1$ are super-critical, while sub-critical systems have $k_{eff} < 1$. Here we should note that Eq. (2.5) is equivalent to Eq. (2.4) only if k_{eff} is strictly equal to one (the system is exactly critical). As discussed before, such systems practically do not exist, so the k-eigenvalue method

[3]Some codes such as MCNP support the α-eigenvalue formulation for steady-state problems [11]. Discussion of the α-eigenvalue formulation is beyond the scope of this thesis.

yields solutions with sufficient accuracy only for systems which are close to critical. For highly sub-critical or super-critical systems, the method can yield considerable errors and other methods should be used instead [12].

To continue the analysis, it is convenient to re-write Eq. (2.5) in operator notation as [13]

$$\mathbf{M} \cdot \psi(\mathbf{r}, \mathbf{\Omega}, E) = \frac{1}{k} \frac{\chi(\mathbf{r}, E)}{4\pi} S(\mathbf{r}), \tag{2.6}$$

where $\mathbf{M}$ denotes the net loss operator defined as

$$\begin{aligned} \mathbf{M} \cdot \psi(\mathbf{r}, \mathbf{\Omega}, E) = \mathbf{\Omega} \cdot \nabla \psi(\mathbf{r}, \mathbf{\Omega}, E) + \Sigma_t(\mathbf{r}, E)\psi(\mathbf{r}, \mathbf{\Omega}, E) - \\ \int_{4\pi} \mathrm{d}\mathbf{\Omega}' \int_0^\infty \mathrm{d}E' \Sigma_s(\mathbf{r}, \mathbf{\Omega}' \to \mathbf{\Omega}, E' \to E)\psi(\mathbf{r}, \mathbf{\Omega}', E'), \end{aligned} \tag{2.7}$$

and $S(\mathbf{r})$ is the fission source

$$S(\mathbf{r}) = \int_{4\pi} \mathrm{d}\mathbf{\Omega}' \int_0^\infty \mathrm{d}E' \nu(\mathbf{r}, E')\Sigma_f(\mathbf{r}, E')\psi(\mathbf{r}, \mathbf{\Omega}', E'). \tag{2.8}$$

It can be further shown [13,14], by applying the Green's function to Eq. (2.6), that an eigenvalue equation, equivalent to Eq. (2.6) can be written just in terms of the fission source

$$S(\mathbf{r}) = \frac{1}{k} \int_V \mathtt{d}\mathbf{r}_0 H(\mathbf{r}_0 \to \mathbf{r}) S(\mathbf{r}_0), \tag{2.9}$$

where the kernel $H(\mathbf{r}_0 \to \mathbf{r})$ is given by

$$\begin{aligned} H(\mathbf{r}_0 \to \mathbf{r}) = \\ \iiiint \mathrm{d}E \mathrm{d}\mathbf{\Omega} \mathrm{d}E_0 \mathrm{d}\mathbf{\Omega}_0 \cdot \nu(E)\Sigma_f(\mathbf{r}, E) \frac{\chi(E_0)}{4\pi} \cdot G(\mathbf{r}_0, E_0, \mathbf{\Omega}_0 \to \mathbf{r}, E, \mathbf{\Omega}). \end{aligned} \tag{2.10}$$

The kernel $H(\mathbf{r}_0 \to \mathbf{r})$ gives the fission source at $\mathbf{r}$ due fission neutrons born at $\mathbf{r}_0$. It corresponds to the Green's function integrated over energies and angles, weighted by the initial spectrum and final fission neutron production [14]. Equations (2.9) and (2.10) can be understood as follows: flux due to fission neutrons born at phase-space point $(\mathbf{r}_0, E_0, \mathbf{\Omega}_0)$ is transformed to the flux at phase-space point $(\mathbf{r}, E, \mathbf{\Omega})$ by the Green's function $G(\mathbf{r}_0, E_0, \mathbf{\Omega}_0 \to \mathbf{r}, E, \mathbf{\Omega})$; multiplying the result with the fission cross section and the average number of fission neutrons $\nu(E)\Sigma_f(\mathbf{r}, E)$, and integrating over the initial and the final energies and angles, as well as the spatial distribution of the initial fission source $\mathbf{r}_0$ gives the new fission source at $\mathbf{r}$.

Finally, introducing an integral fission operator F to the right-hand side of Eq. (2.9), the source eigenvalue equation can be written as

$$S = \frac{1}{k} F S. \tag{2.11}$$

Monte Carlo criticality calculation can be understood as an iterative procedure equivalent to the procedure for determining the fundamental eigenpair of operator

F in Eq. (2.11), $k_0 = k_{eff}$ and $S_0(\mathbf{r})$. The procedure to find the fundamental eigenpair of linear eigenproblems such as Eq. (2.11) is commonly adopted as the power iteration scheme [15]

$$S^{(i+1)} = \frac{1}{k^{(i)}} F S^{(i)}, \tag{2.12}$$

where

$$k^{(i)} = \frac{\int_V \mathrm{d}\mathbf{r} F S^{(i)}}{\int_V \mathrm{d}\mathbf{r} S^{(i)}}. \tag{2.13}$$

The power iteration is known to always converge to the fundamental eigenpair if the largest eigenvalues are not of equal magnitude [16].

During each iteration cycle (so-called criticality cycle), Monte Carlo codes sample m neutrons from the fission sites corresponding to $S^{(i)}$ and simulate their transport through the system to determine the fission sites for the next-generation source $S^{(i+1)}$. The initial source distribution $S^{(0)}$ and the eigenvalue $k^{(0)}$ are guessed. The procedure is repeated n times, while $h = \sum_{i=0}^{n} m_i$ gives the total number of neutron histories simulated. Because the source is sampled at a finite number of fission sites, m, the Monte Carlo equivalent of Eq. (2.12) includes the statistical error term ϵ [17, 18], i.e.

$$S^{(i+1)} = \frac{1}{k^{(i)}} F S^{(i)} + \epsilon^{(i)}. \tag{2.14}$$

The statistical error in the fission source is of order $O(1/\sqrt{m})$, while the expected value of the statistical error is assumed as $E[\epsilon^{(i)}] = 0$. Since the results from a Monte Carlo criticality calculation are combined over a number of cycles, the total error of Monte Carlo results would decrease as $O(1/\sqrt{h})$ after the fundamental mode has established, if no systematic errors exist. This will be elaborated in the following section.

2.4 Fission Source Convergence

The fission source, given by Eq. (2.12), can be expressed as a weighted sum of the eigenfunctions S_j as

$$S^{(n)} = F^n \sum_j a_j S_j = \sum_j a_j k_j^n S_j, \tag{2.15}$$

where a_j are used as arbitrary weighting factors. If the eigenvalues are arranged in a descending order i.e. $k_0 > |k_1| > |k_2| > \ldots$ and Eq. (2.15) is divided by k_0^n to obtain

$$\frac{S^{(n)}}{k_0^n} = a_0 S_0 + \left(\frac{k_1}{k_0}\right)^n a_1 S_1 + \left(\frac{k_2}{k_0}\right)^n a_2 S_2 + \ldots, \tag{2.16}$$

we can see that the power iteration will converge to the fundamental mode S_0 at the limit of $n \to \infty$, if $k_0 \neq k_1$. We can further see that $1 > |k_1/k_0| > |k_2/k_0| \ldots$, so $S^{(n)}$

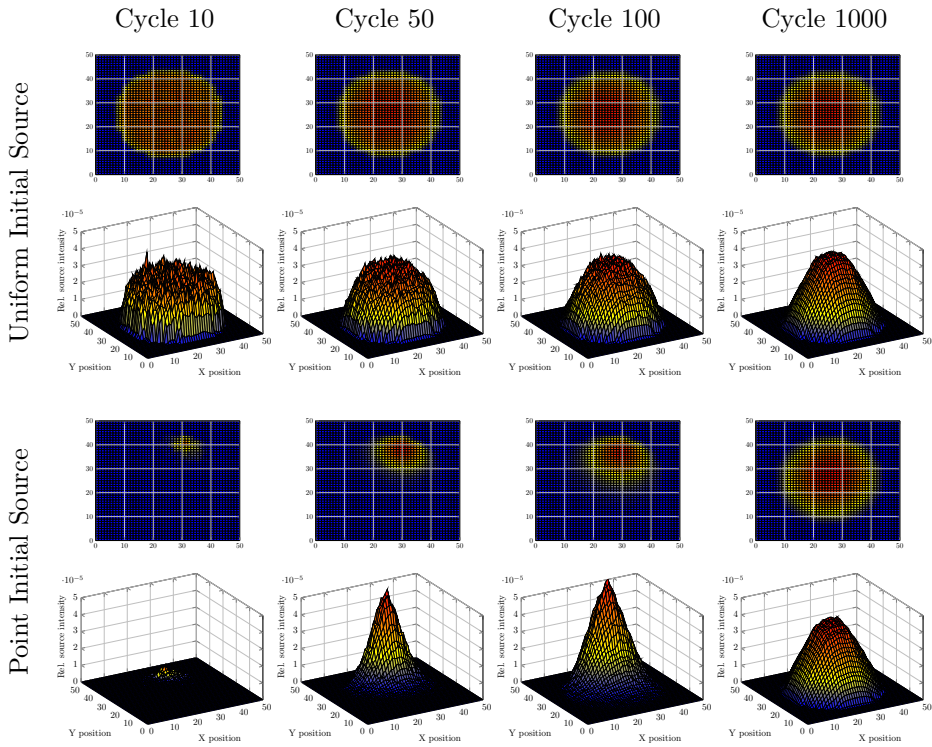

Figure 2.2: Convergence of the fission source in Monte Carlo criticality calculations.

converges to S_0 as $O((k_1/k_0)^n)$. This analytical argument following from the basis of the power method [16,18] was confirmed for Monte Carlo criticality calculations as well [19]. The ratio k_1/k_0 is known as the dominance ratio of the system, hence systems with dominance ratio close to unity exhibit slow fission source convergence.

Monte Carlo criticality simulations are started from some initial guess of the fission source distribution, which introduces an initial error compared to the fundamental mode source distribution. The results collected using this source would be subject to the initial error as well. Since the initial guess converges to the fundamental mode as $O((k_1/k_0)^n)$, the initial error decreases at the same rate. Eventually, after a certain number of iterations, the initial error would decay to an extent where the fission source may be considered to approximate the fundamental mode sufficiently well. Such iterations are called *inactive cycles*; no results are collected during the inactive cycles. The results are collected during the *active cycles*, i.e. the cycles when the fission source distribution is assumed to be converged to the fundamental mode.

Because the Monte Carlo fission source is sampled at a finite number of sites, it

contains a statistical error of order $O(1/\sqrt{m})$. It was noticed, that error propagation through the iteration cycles causes the fission source to converge to a biassed distribution $\hat{S}_0$ compared to the fundamental mode distribution S_0. The difference between S_0 and $\hat{S}_0$ was shown to be $O(1/m)$ [20]. The biassed distribution tends to underestimate the fission source in the most reactive regions of the system and overestimate the source in less reactive regions [21]. Hence, the fundamental eigenvalue, k_{eff}, estimated from the biassed source is usually smaller than the correct one.

Fission source convergence is illustrated in Figure 2.2. Here we show the cumulative fission source, i.e. the source combined over all previous simulation cycles. The figure depicts two cases with the source sampled from the uniform and point initial distributions. The statistical error can be seen as the noise in the distribution, while the distribution converges to the fundamental mode with increasing cycle number. The calculation was performed using the PWR performance benchmark model [6] and Serpent 2 reactor physics code [5].

2.5 Improving Monte Carlo Criticality Calculations

In the previous section, we established that Monte Carlo criticality calculations consist of a number of inactive and active cycles where the inactive cycles are necessary to converge the fission source to the fundamental mode. Since no results are collected during the inactive cycles, these cycles increase the overall computing cost of Monte Carlo criticality calculations. Moreover, the fission source may be subject to bias, which can corrupt the results.

Various approaches were previously proposed to address these issues, such as the superhistory powering method [20], the Wielandt method [22], as well as a number of methods driven by deterministic calculations, e.g. [23]. In this section, we will discuss several methods that aim at improving the efficiency of Monte Carlo criticality calculations by either providing a better initial estimate of the fission source distribution through the use of fission or response matrices or by optimizing the number of neutrons simulated. Subsections 2.5.1 and 2.5.2 establish the concepts of fission and response matrices, which will be relevant in the discussion on time-dependent methods in Chapter 3. Subsection 2.5.3 summarizes the previous work related to the method described in Paper I.

2.5.1 Fission Matrix Methods

Fission matrix corresponds to a space-discretized fission operator F. The k-eigenvalue problem is discretized into N spatial regions and Eq. (2.9) or Eq. (2.11) is integrated over the volumes, V, of each initial region j, with $\mathbf{r_0} \in V_j$ and final region i, with $\mathbf{r} \in V_i$. The fission source in region i can then be expressed as [13, 14]

$$S_i = \frac{1}{k} \sum_{j=1}^{N} F_{i,j} \cdot S_j, \tag{2.17}$$

or in a matrix-vector form as

$$\mathbf{S} = \frac{1}{k}\mathbb{F} \cdot \mathbf{S}, \tag{2.18}$$

where matrix $\mathbb{F}$ is called the fission matrix. The elements of the fission matrix $F_{i,j}$ represent the expected number of fission neutrons born in region i due to one fission neutron starting in region j, which can be formally expressed as [13, 14]

$$F_{i,j} = \int_{\mathbf{r}\in V_i} \mathrm{d}\mathbf{r} \int_{\mathbf{r}_0\in V_j} \mathrm{d}\mathbf{r}_0 \frac{S(\mathbf{r}_0)}{S_j} \cdot H(\mathbf{r}_0 \to \mathbf{r}), \tag{2.19}$$

with

$$S_j = \int_{\mathbf{r}'\in V_j} S(\mathbf{r}')\mathrm{d}\mathbf{r}'. \tag{2.20}$$

The elements of the fission matrix can be estimated during the n^{th} cycle of a Monte Carlo criticality calculation as [21]

$$F^{*(n)}_{i,j} = f^{*(n)}_{i,j}/s^{(n-1)}_j, \tag{2.21}$$

where $f^{*(n)}_{i,j}$ is used to denote the total expected number of fission neutrons in zone i, during cycle n produced by neutrons originating from zone j, during cycle $n-1$, and $s^{(n-1)}_j$ is the number fission neutrons from cycle $(n-1)$ in zone j. The estimation of the matrix elements can then be combined over n simulated cycles as [21]

$$F^{(n)}_{i,j} = f^{(n)}_{i,j}/t^{(n-1)}_j, \tag{2.22}$$

where

$$f^{(n)}_{i,j} = \sum_{l=1}^{n} f^{*(l)}_{i,j}, \tag{2.23}$$

$$t^{(n-1)}_j = \sum_{l=1}^{n} s^{(l-1)}_j. \tag{2.24}$$

Fission matrix condenses valuable information about the system, which can be used in various ways. Initially, it was assumed that the fundamental mode eigenvector of the fission matrix would converge faster than the Monte Carlo fission source, hence Monte Carlo fission source convergence acceleration techniques based on the fundamental mode eigenvector of the fission matrix were proposed [24]. However, stability and convergence problems of these methods were identified [21, 25], while the authors observed that the fission matrix becomes insensitive to errors in the Monte Carlo fission source if sufficiently small node size is used. Indeed, it was shown that at the limit of small node size, the fission matrix becomes independent on the phase-space weighting of the matrix elements [13]. Correlation of errors between the Monte Carlo fission source and the fundamental eigenvector of the fission matrix were also studied [26], where it was concluded that the correlation reduces when the node size is decreased.

Furthermore, the fission matrix may be used to calculate higher-order forward and adjoint system eigenpairs [13]. Hence, the fission matrix may be used as direct means of performing criticality analyses in so-called fission matrix-based Monte Carlo criticality calculations [21, 27–29]. The method was later expanded to time-dependent problems [30], which will be discussed in Section 3.3.

2.5.2 Response Matrix Methods

Similarly to the fission matrix methods, the Response Matrix Methods (RMMs) are based on a variant of the Green's function approach. However, here a number of Green's functions are defined for each sub-volume of the system, differently from the fission matrix methods where a single, discretized Green's function is used to describe the entire system. Specifically, the RMMs discretize a large, global spatial domain (such as a reactor core) to a number, N, of non-overlapping local sub-domains (nodes) which are coupled through partial currents [31–33]. Then, the neutron transport problem is solved by constructing the global solution from a set of precomputed solutions to the local problems in the sub-domains. Because the response of a node depends only on the properties of that node, the local problem needs to be solved only for the unique nodes [34], provided that the boundary conditions on the node are well represented. Hence, the RMMs become efficient if many of the nodes constituting the original problem have identical geometrical shape and material composition [32, 34, 35].

Response matrix methods relate the partial currents outgoing from node i, j_i^+, with the partial currents incoming to the node, j_i^-, through response kernels R_i as [31]

$$j_i^+(\mathbf{r}) = \int_{S_i} R_i(\mathbf{r}' \rightarrow \mathbf{r}) j_i^-(\mathbf{r}') \mathrm{d}\mathbf{r}', \tag{2.25}$$

where the integration is carried over the entire node surface S_i and other phase-space variables $(\mathbf{\Omega}, E)$ were suppressed for now and will be discussed later. The discussion of the time variable is left for Section 3.4. The response kernels R_i $(i = 1, 2, ..., N)$ depend only on the properties of node i, and are assumed to be known from independent solutions of the local problems. The kernels can be calculated by applying diffusion or transport theories [31, 32, 36, 37], or can be sampled using the Monte Carlo method [35, 38–45].

The individual nodes are then coupled together through partial currents, to solve the global problem. If the partial currents are expressed as a column vector

$$\mathbf{J}^{\pm} = [j_1^{\pm}, j_2^{\pm}, ..., j_N^{\pm}]^T, \tag{2.26}$$

Eq. (2.25) takes a compact form

$$\mathbf{J}^+ = \mathbb{R}\mathbf{J}^-. \tag{2.27}$$

Here $\mathbb{R}$ is a block-diagonal matrix where each block represents the kernel R_i of node i. Because each node has common boundaries with the neighbouring nodes,

the outgoing partial currents immediately become incoming partial currents for the neighbours, so

$$\mathbf{J}^{-} = \mathbb{M}\mathbf{J}^{+}, \tag{2.28}$$

where $\mathbb{M}$ is the connectivity matrix, which redirects the outgoing currents to incoming currents of the neighbours and includes the global domain boundary conditions. Then, combining Eqs. (2.27) and (2.28) leads to the response matrix equations for the global domain:

$$\mathbf{J}^{+} = \mathbb{R} \cdot \mathbb{M}\mathbf{J}^{+}. \tag{2.29}$$

Depending on the formulation of the method, fission can be treated either implicitly, using the so-called "direct" RMM, or explicitly, using the so-called "source" RMM [31, 32, 37]. In the direct RMM formulation, the response kernels are calculated as functions of the multiplication factor, k, and if no volumetric information is desired, only surface to surface calculations need to be performed [39]. To solve a criticality problem, Eq. (2.29) is written as a non-linear eigenvalue equation

$$\lambda\mathbf{J}^{+} = \mathbb{R}(k) \cdot \mathbb{M}\mathbf{J}^{+}, \tag{2.30}$$

where λ is the current eigenvalue that represents the global balance of neutron currents through all nodal surfaces. If the response matrix $\mathbb{R}(k)$ strictly maintains neutron balance, the value of λ approaches unity as k approaches k_{eff} [37].

In the source RMM formulation, separate response kernels are defined for the surface-to-surface, surface-to-volume, volume-to-surface, and volume-to-volume responses [31, 38, 40, 42, 43, 45]. The response matrix equations then take the general form of

$$\mathbf{J}^{+} = \mathbb{R}^{ss} \cdot \mathbb{M}\mathbf{J}^{+} + \mathbf{J}^{+}_{\mathbf{f}}, \tag{2.31}$$

where $\mathbb{R}^{ss}$ contains surface-to-surface responses and $\mathbf{J}^{+}_{\mathbf{f}}$ denotes the outgoing partial currents due to volume sources in the nodes. $\mathbf{J}^{+}_{\mathbf{f}}$ can be evaluated knowing the volume-to-surface response matrix $\mathbb{R}^{vs}$ as

$$\mathbf{J}^{+}_{\mathbf{f}} = \mathbb{R}^{vs}\mathbf{Q}, \tag{2.32}$$

were $\mathbf{Q}$ denotes the volume sources, which are calculated knowing the volume-to-volume and surface-to-volume response matrices $\mathbb{R}^{vv}$ and $\mathbb{R}^{sv}$ as

$$\mathbf{Q} = \mathbb{R}^{sv} \cdot \mathbb{M}\mathbf{J}^{+} + \mathbb{R}^{vv}\mathbf{Q}. \tag{2.33}$$

The criticality problem can then be solved using some iterative scheme based on Eqs. (2.31) and (2.33), and scaling the volume sources by k among iterations.

In Eq. (2.25), the integration was carried over the entire surface of the node. Assuming each node has n neighbours (e.g. $n = 6$ in 3D Cartesian geometry), the node surface S_i can be partitioned to n sub-surfaces (faces), $S_{i,k}$ $(k = 1, 2, ..., n)$. Then, each block of matrix $\mathbb{R}$, R_i, becomes a $n \times n$ matrix, where each element describes the outgoing current response (on n faces), due to incoming currents (on

n faces). The vectors $\mathbf{J}^{\pm}$ then consist of sub-vectors, which contain the partial currents on each face of the node, $j^{\pm}_{i,k}$.

If the entire system is to be represented by a limited number of local solutions for the unique nodes, some means are necessary to represent the dependence of the boundary conditions on the phase-space variables, as Eq. (2.25) takes the form of

$$j^{+}_{i}(\mathbf{r},\mathbf{\Omega},E) = \iiint R_i(\mathbf{r}',\mathbf{\Omega}',E' \rightarrow \mathbf{r},\mathbf{\Omega},E) j^{-}_{i}(\mathbf{r}',\mathbf{\Omega}',E')\mathrm{d}\mathbf{r}'\mathrm{d}\mathbf{\Omega}'\mathrm{d}E'. \tag{2.34}$$

This is achieved by projecting the phase-space variables $\mathbf{r}$, $\mathbf{\Omega}$, and E onto various finite sub-spaces represented by some orthogonal basis, defined on each face of the node [31, 36, 37]. Assuming that the phase-space $\mathbf{w} = (\mathbf{r},\mathbf{\Omega},E)$ can be represented by a basis $P_l(\mathbf{w})$, and the expansion is truncated at some order L, the partial currents become [37]

$$j^{\pm}_{i,k}(\mathbf{w}_{i,k}) \approx \sum_{l=0}^{L} j^{\pm}_{i,k,l} P_l(\mathbf{w}_{i,k}), \tag{2.35}$$

where $j^{\pm}_{i,k,l}$ denote the expansion coefficients. The partial currents are then represented by the expansion coefficients and the global current vector $\mathbf{J}^{\pm}$ becomes of size $N \cdot n \cdot (L+1)$ [31].

The response kernels are expressed using the same basis and each block of the global response matrix $\mathbb{R}$ becomes of size $[(L+1)n] \times [(L+1)n]$ [31], where the block elements $r^{k,l}_{i,k',l'}$ characterize the l-th order outgoing current response on surface k due to an incoming l'-th order current on surface k', of node i [37]:

$$r^{k,l}_{i,k',l'} = \int j^{+}_{i,l'}(\mathbf{w}_{i,k}) P_l(\mathbf{w}_{i,k'})\mathrm{d}\mathbf{w}_{i,k'}. \tag{2.36}$$

The accuracy of the approximation and the required computing effort depends on the selected basis functions and expansion orders. Weiss and Lindahl [31] used Legendre polynomials up to the 4-th order to represent the spatial variables and argued that the 1-st order expansion is sufficient for practical problems. Forget [39] used a tensor product of Legendre polynomials in attempt to represent the entire phase-space ($\mathbf{r}$,$\mathbf{\Omega}$,E). Various combinations of expansion orders were tested using a multi-group energy representation and the author concluded that the low order expansions give accurate results for 2D problems, but this feature is not retained for 3D problems. In recent publications on the COMET method [35, 44], the authors use a tensor product of Legendre and Chebyshev polynomials, where Legendre polynomials are used for the spatial variables (in 2D) and the azimuthal angle, and the Chebyshev polynomials are used for the cosine of the polar angle; the authors then argue that expansions up to 4-th order in space and up to 2-nd order in angle with a multi-group energy representation are sufficient for a wide variety of reactors, while a direct extension of the method to the continuous energy variable would require more than 1000-th expansion order and thus is impractical.

In a recent publication, Leppänen [46] proposed using the response matrix method for acceleration of fission source convergence in Monte Carlo criticality calculations. The proposed approach is similar to the fission matrix acceleration methods; the response kernels for all nodes in the system are estimated during a Monte Carlo criticality simulation of the entire system, then an improved guess of the fission source distribution is obtained from the solution of the response matrix equations. Since the response matrix methods couple each node only to the neighbouring nodes, the approach offers better scaling compared to the fission matrix methods, where each node is coupled to all other nodes in the system. Moreover, the response kernels are calculated using the angular flux representative of each part in the system, so the expansions to represent the phase-space dependence become not necessary, which greatly simplifies the formulation of the response matrix equations.

2.5.3 Optimization of Neutron Population Size

In the previous two sections, we discussed two fission source convergence acceleration methods that aim to obtain an improved estimate of the fission source distribution through the use of fission or response matrices. Scoring the information necessary to provide the improved estimate may, in some cases, be as computationally expensive as the simulation with no acceleration, because the number of particles simulated during one cycle (the neutron population size) may need to be significantly increased. Hence, these methods may indeed reduce the number of inactive cycles required to obtain a converged fission source, but may not necessarily reduce the overall computing cost of a Monte Carlo criticality calculation.

Monte Carlo criticality calculations are commonly conducted by simulating a number of source iteration cycles using a fixed number of source neutrons during each cycle. The computing cost of such calculations is directly proportional to the selected number of neutrons and iteration cycles, i.e. the total number of simulated neutron histories, h. Hence, the calculation efficiency can be expressed in terms of the figure-of-merit, FOM, defined through h as

$$FOM = \frac{1}{\epsilon^2 h}, \tag{2.37}$$

where ϵ is the error in the results. A more efficient calculation thus can be achieved by either lowering the error (using methods described before) without significantly increasing the computing cost (without simulating more neutrons) or reducing the computing cost (by simulating fewer neutrons) necessary for achieving the same error value.

In Section 2.4, we discussed that the error in Monte Carlo criticality calculation results can be decomposed into three components: the initial error of $O((k_1/k_0)^n)$, the error caused by bias of $O(1/m)$, and the statistical error of $O(1/\sqrt{h})$. Selecting a small neutron population size (the number of neutrons simulated per cycle) could lower the computing cost of Monte Carlo criticality calculations; however,

a considerable bias could be introduced in the fission source this way. While the initial error and the statistical error decay over the simulation cycles, the bias does not decay and eventually may dominate the total error. Therefore, a large neutron population size is commonly preferred to assure that the results are not affected by the source bias [47]. On the other hand, large population size increases the computing time of a single cycle, thus limiting the number of cycles which can be simulated in certain computing time. Tuttelberg and Dufek [48] recognised this as a population size optimization problem and proposed a methodology to optimize the batch size in Monte Carlo criticality calculations.

In subsequent research [49], the authors suggested increasing the population size throughout the simulation cycles. This way, at any cycle in the simulation, the neutron population size is kept small enough for efficient source iteration, while at the same time large enough for limiting the source bias. Since the initial and the statistical errors dominate the total error at the beginning of a simulation, large initial population size is unnecessary for assuring a small value of the source bias; as the errors decay in the successive cycles, the population size is increased, reducing the source bias. The proposed algorithm divides the calculation into stages, where at each stage the population size is increased based on the error estimated using the fundamental-mode eigenvector of a fission matrix. The fission matrix is scored during the simulation, and the fundamental-mode eigenvector of the matrix is computed at each simulation stage.

Scoring the fission matrix and calculating the fundamental-mode eigenvector constitutes additional computing overhead, which may prevent an efficient application of the method to large-scale problems, where a fine mesh resolution for the fission matrix may be required. Then, the computing overhead associated with the on-the-fly error estimation may reduce the overall efficiency gain. Paper I suggests a method for determining the batch size using a simple analytical relation. This way, the overhead associated with tallying the fission matrix and computing the fundamental-mode eigenvector can be eliminated.

Chapter 3

Time-Dependent Problems

This chapter is intended to provide the background material supporting Paper II. First, the concepts of time-dependent reactor analyses are introduced. Then, the recent developments of three Monte Carlo based time-dependent methods are overviewed: the Time-Dependent Monte Carlo (TDMC) method, the Transient Fission Matrix (TFM) method, and the Time-Dependent Response Matrix (TDRM) method. The TDMC method relies exclusively on Monte Carlo techniques, while the TFM and the TDRM methods use various Green's functions approaches. Information necessary for the TFM and the TDRM methods can be obtained from steady-state Monte Carlo calculations.

3.1 Time-Dependent Reactor

The time-dependent transport equation presented in Section 2.1 implies that all fission neutrons are *prompt* neutrons emitted instantaneously in fission events. However, it is known that a small fraction ($\sim 0.2 - 0.7$ %) of all fission neutrons are *delayed* neutrons emitted after a considerable time delay ranging from less than a second to more than a minute [3]. Emission of delayed neutrons follows the decay of some of the fission products, known as delayed neutron *precursors*. The fraction of delayed neutrons is commonly denoted by β; it depends on the fissioning nuclide and the energy of the neutron inducing fission.

The presence of delayed neutrons significantly changes the time behaviour of a nuclear system. Indeed, if only prompt neutrons were present, power in a super-critical system would increase at a rate proportional to the prompt neutron lifetime $l \sim 10^{-7}$–10^{-4} s. Effective control of such a system would be complicated at best. The presence of delayed neutrons considerably prolongs the time-scale associated with power changes, which ensures that power can be effectively controlled by mechanical means, such as control rods. The latter holds if the system is so-called *delayed super-critical* meaning that the neutrons contributing to increase of power are delayed neutrons.

For practical purposes, the delayed neutron precursors are commonly divided into six or eight groups. The expected density of precursors in the j^{th} group is denoted as $C_j(\mathbf{r},t)$ with a corresponding decay constant λ_j. The expected rate of delayed neutron emission from this group is then given by the decay rate of the precursors in that group, $C_j\lambda_j$. If the delayed neutron fraction coming from the decay of j^{th} group precursors is denoted as β_j, the total fraction of delayed neutrons is obtained by adding all of the group fractions, $\beta = \sum_j \beta_j$. Hence, out of all fission neutrons, $\beta\nu$ neutrons will appear as delayed neutrons and $(1-\beta)\nu$ will appear as prompt neutrons.

To reflect the presence of delayed neutrons, we modify the fission term and introduce the delayed neutron term into the transport equation (Eq. (2.4)) to obtain

$$\begin{aligned}\frac{1}{v}\frac{\partial}{\partial t}\psi(\mathbf{r},\mathbf{\Omega},E,t) + \mathbf{\Omega}\cdot\nabla\psi(\mathbf{r},\mathbf{\Omega},E,t) + \Sigma_t(\mathbf{r},E,t)\psi(\mathbf{r},\mathbf{\Omega},E,t) = \\ q_{ex}(\mathbf{r},\mathbf{\Omega},E,t) + \int_{4\pi}\mathrm{d}\mathbf{\Omega}'\int_0^\infty \mathrm{d}E'\Sigma_s(\mathbf{r},\mathbf{\Omega}'\to\mathbf{\Omega},E'\to E,t)\psi(\mathbf{r},\mathbf{\Omega}',E',t) + \\ \frac{\chi_p(\mathbf{r},E)}{4\pi}\int_{4\pi}\mathrm{d}\mathbf{\Omega}'\int_0^\infty \mathrm{d}E'(1-\beta(\mathbf{r},E'))\nu(\mathbf{r},E')\Sigma_f(\mathbf{r},E',t)\psi(\mathbf{r},\mathbf{\Omega}',E',t) + \\ \frac{1}{4\pi}\sum_j \lambda_j C_j(\mathbf{r},t)\chi_{d,j}(\mathbf{r},E),\end{aligned} \tag{3.1}$$

where χ was replaced by χ_p, which denotes the energy spectrum of prompt neutrons, and $\chi_{d,j}$ denotes the energy spectrum of delayed neutrons born in group j. Percursor concentrations in Eq. (3.1) can be expressed by considering ballances for each precursor group C_j as [2]

$$\begin{aligned}\frac{\partial C_j(\mathbf{r},t)}{\partial t} + \lambda_j C_j = \\ \int_{4\pi}\mathrm{d}\mathbf{\Omega}'\int_0^\infty \mathrm{d}E'\beta_j(\mathbf{r},E')\nu(\mathbf{r},E')\Sigma_f(\mathbf{r},E',t)\psi(\mathbf{r},\mathbf{\Omega}',E',t),\end{aligned} \tag{3.2}$$

where the term on the right-hand side describes the expected rate of j^{th} group precursor production.

The various cross-sections in Eqs. (3.1) and (3.2) are now functions of time indicating possible changes due to feedbacks, movement of control rods, or changes in fuel composition. The effects of changes in fuel composition are addressed in so-called *burnup* analyses. Fuel burnup occurs over long time intervals, hence the short-time effects, like that of delayed neutrons, are commonly excluded from such analyses and the system is assumed to be in steady-state. In this chapter, we will focus on short-term reactor transients, where the effect of delayed neutrons has to be considered. Analysis of reactor transients irrespective of the source for the feedbacks is known as *reactor kinetics*. In *reactor dynamics* analyses the sources of feedbacks are considered explicitly, which requires coupling of neutronics models to e.g. thermal-hydraulics models for a multi-physics description of the system.

Solving Equations (3.1) and (3.2) would yield the time behaviour of the angular neutron flux taking into account the effect of delayed neutrons. However, a direct numerical solution is prohibitive as discussed in Section 2.1, and various approximations to neutron transport are introduced to simplify the problem. Here, the problem is complicated further by the presence of two time-scales for prompt and delayed neutrons. Common deterministic approaches include flux factorisation into slow and fast-varying components, as in quasi-static and adiabatic methods, use of the point-kinetics model, or formulation of simplified time-dependent transport or diffusion models, combined with appropriate numerical techniques to resolve the two time-scales.

3.2 Time-Dependent Monte Carlo Method

Extension of steady-state Monte Carlo methods to time-dependent methods is conceptually straight-forward since time is implicitly present in a Monte Carlo simulation of a particle history. Correspondingly, the first ideas to apply Monte Carlo methods to simulate time-dependent neutronics problems were proposed multiple decades ago [50]. However, development of Time-Dependent Monte Carlo (TDMC) methods for transient analyses of nuclear systems was limited until fairly recently, when access to significant computing power required for such analyses became widely available [51–53]. Currently, various implementations of time-dependent Monte Carlo solvers are discussed in literature [54–62], with attempts to couple the Monte Carlo reactor kinetics with thermal-hydraulic feedbacks for solving dynamic problems [63, 64].

TDMC methods rely exclusively on Monte Carlo techniques, thus avoiding the approximations used in deterministic methods. No simplifications are made to neutron transport; similar to stationary Monte Carlo simulations, each neutron history is treated by explicitly following the fundamental interaction laws. The phase-space is not discretized, in contrast to diffusion, S_n, or P_n theories applied in deterministic methods (see e.g. [2, 33]). Moreover, each neutron within a fission chain is tracked explicitly in time, differently from Monte Carlo criticality calculations where the neutrons are tracked cycle-by-cycle from birth to death. This results in no separation between space and time, as in quasi-static and other deterministic methods which rely on factorization techniques (see e.g. [2, 65]).

Simulating nuclear reactor transients by a Monte Carlo process poses challenges due to presence of delayed neutrons and emission of multiple neutrons during fission in so-called fission chain branching [4, 53, 54]. Large time-scale differences between prompt neutron chains and delayed neutron emissions yield considerable delay between the subsequent delayed neutron-induced fission chains, which in turn results in a high variance of the results. Branching of neutron chains during fission events causes a significant spread in the neutron chain lengths and consequently yields high variance of the results as well.

High variance in TDMC simulations of nuclear reactor transients means that

a large number of samples has to be collected for acceptable statistical accuracy. This yields prohibitive computing time, especially for large-scale problems, such as full-core transient analysis. Computing times ranging from a couple of hundreds of CPU hours (for small kinetics problems in simple geometries) to multiple thousands of CPU hours (for problems in assembly and mini-core geometries) were reported [4, 62,63]. Such computing times would extrapolate to multiple CPU years for realistic large-scale problems with feedbacks. Therefore the TDMC method is primarily intended to benchmark less computationally expensive tools and for investigating unique reactor designs and concepts [4, 54], while methods to reduce the required computing effort are being pursued [4, 62].

Main aspects of the TDMC method are elaborated in the following sections. First, the procedure of tracking in time is described. Then, several methods proposed for treating the delayed neutrons, performing population control, and variance reduction are overviewed.

3.2.1 Tracking in Time

The time variable is explicitly present in TDMC calculations, in contrast to criticality or fixed source Monte Carlo calculations where the events are recorded independently of their time of occurrence. Here, the overall calculation time is split into time intervals which are used to score the quantities of interest, introduce system feedbacks, perform population control, or adjust other calculation parameters (e.g. weight windows) [54]. The time intervals can be non-uniform, and different sets of intervals can be used for different tasks, e.g. quantity scoring or population control [62].

Differently from deterministic methods, where the size of a time step can numerically influence the accuracy of the calculation results, the sizes of the time intervals in a TDMC calculation only determine the sizes of the tally bins and therefore the resolution in which the tallied quantity is represented [54]. Here, the bin value corresponds to the time integral of the corresponding Monte Carlo score [62].

The time variable is treated by simply assigning a time parameter (the "internal clock") for each transported particle. The clock is set to zero at the start of the simulation and is progressively updated during the particle's history, as

$$t_i = t_{i-1} + \frac{s_i}{\sqrt{2E_i/m}}, \tag{3.3}$$

where s_i is the i-th free path length, E_i and m are the energy and the mass of the particle respectively. If the particle crosses the time interval boundary, it is stopped exactly at the boundary and a new path length (together with the corresponding flight time) is sampled with (possibly) updated cross-sections.

Because of the Markovian nature, the simulation of particle trajectories can be stopped and restarted at the time interval boundaries without changing the statistical features of the transport process [54,62]. The TDMC simulation is performed on an interval-by-interval basis, where the surviving particles are stored for the

next time interval. All primary and secondary particles within a time interval will either die (through absorption and leakage) or survive by crossing the time interval boundary.

3.2.2 Treatment of Delayed Neutrons

Delayed neutrons can, in principle, be treated in an analog way in a TDMC simulation [56, 57]; however, different time-scales between the lifetime of a neutron in a reactor (from 10^{-7} s in a fast reactor to 10^{-4} s in a thermal reactor), the lifetime of prompt neutron chains (from 10^{-5} s to 10^{-2} s respectively), and emission of delayed neutrons (from 10^{-2} s to 10^{2} s for different precursor groups) introduce large variance to the results [4, 53, 54]. Because the number of particles in a Monte Carlo simulation is always limited (due to limitations in CPU time and memory), the two different timescales present in the simulation result in long time intervals with no delayed neutrons to initiate new prompt neutron chains. Hence, the neutron population significantly fluctuates in time, causing large variance in the scored quantities. In a real system, this effect is averaged out by a very large number of delayed neutron precursors and independent concurrent prompt neutron chains [54].

To overcome this limitation a "forced precursor decay" method was proposed [4, 53,54]. Here, all precursor families are combined into a single "combined precursor" particle. The decay probability of the combined precursor is then given by

$$P_c(t) = \sum_i f_i \lambda_i \mathrm{e}^{-\lambda_i (t-t_0)}, \tag{3.4}$$

where t_0 is the time when the precursor was created and f_i is the normalized fraction of delayed neutrons originating from the i-th precursor family,

$$f_i = \frac{\beta_i}{\beta}. \tag{3.5}$$

Then, a part of the combined precursor particle weight is forced to decay during each time interval, Δt, of the simulation. The precursor decay time is sampled uniformly within the time interval from the uniform probability density function

$$P_d = \frac{1}{\Delta t}. \tag{3.6}$$

The bias introduced by such procedure is compensated by adjusting the statistical weight of the resulting delayed neutron as

$$w_d = w_c \frac{P_c(t)}{P_d(t)} = w_c \Delta t \sum_i f_i \lambda_i \mathrm{e}^{-\lambda_i (t-t_0)}, \tag{3.7}$$

where w_c is the initial weight of the combined precursor.

The energy distribution of delayed neutrons is different from that of prompt neutrons. Therefore, the energy of a delayed neutron should be sampled from the energy distribution corresponding to the precursor group which yielded the delayed neutron. Because all precursor groups are combined into a single combined precursor particle, the probability of sampling from group i changes with time as

$$P_i(t) = \frac{f_i \lambda_i \mathrm{e}^{-\lambda_i (t-t_0)}}{\sum_j f_j \lambda_j \mathrm{e}^{-\lambda_j (t-t_0)}}. \tag{3.8}$$

The forced precursor decay method ensures that delayed neutrons are present in each time interval to initiate the prompt neutron chains. After sampling the emission time within a time interval according to Eq. (3.6), the weight of the delayed neutron is calculated according to Eq. (3.7), and the energy is sampled from the distribution according to the precursor group selected using Eq. (3.8). The delayed neutron transport is then simulated within the current time interval, and the precursor is not killed but added to the buffer of particles for the next time interval.

The forced decay method can be also be applied without combining all precursor families into a single particle and treating each precursor group explicitly as reported in refs. [61, 64, 66]. The authors in [61] argue for such an approach by claiming that the way to assign weights to the different groups of precursors is not unique.

3.2.3 Population Control

In TDMC calculations, the population would either exponentially grow in a super-critical system or decay in a sub-critical system. Consequently, methods to maintain the population close to the starting number of particles are desired. Convenient points in the simulation to perform population control are the time interval boundaries. The time intervals used for population control can be non-uniform and may be different from the time intervals used for scoring the quantities of interest, as discussed in Sec. 3.2.1. One should also consider that the population might diverge within a time interval in a super-critical system, or disappear within a time interval in a sub-critical system. Therefore, while the choice of time intervals is arbitrary in principle, the population control restricts this choice in practice [62].

Two different populations need to be controlled in TDMC calculations: the population of precursors and the population of neutrons. Combing method [4, 62] and Russian roulette/splitting [4, 54] techniques were applied for population control in non-analog simulations, while techniques to discard or double random particles were applied in analog simulations [56, 57].

Application of Russian roulette technique for the neutron population is performed in several steps [4]. First, the desired average population weight is deter-

mined as

$$W_{av} = \frac{1}{N}\sum_{i=1}^{M} w_i, \tag{3.9}$$

where N is the initial number of neutrons, and the summation is over the weights, w_i, of M particles stored at the end of the previous time interval. The Russian roulette is then applied for all neutrons having the weight lower than the threshold set as

$$W_{RR} = w_{RR} W_{av}, \tag{3.10}$$

where w_{RR} is the relative threshold (w_{RR} values of 0.25 and 0.8 were used in [4]). Finally, the survival probability is calculated as

$$P_{surv} = \frac{w}{W_{av}}. \tag{3.11}$$

If the neutron survives, its weight after the roulette, w', is set as

$$w' = W_{av}. \tag{3.12}$$

Using the forced precursor decay method (see Sec. 3.2.2), the precursor population will increase over time because all precursors are stored for the next time interval. On the other hand, the weight of delayed neutrons emitted from the stored precursors will decrease over time (see Eq. (3.7)). Sjenitzer and Hoogenboom [4,54] suggest to use the "expected weight" of a delayed neutron for precursor population control. The expected weight, $w_{n,ex}$, is the weight of a delayed neutron to be emitted in the next time interval:

$$\begin{aligned} w_{n,ex} &= \frac{w_c}{\Delta t}\int_{t_1}^{t_1+\Delta t} \Delta t \sum_i f_i \lambda_i \mathrm{e}^{-\lambda_i (t-t_0)} \mathrm{d}t \\ &= w_c \sum_i f_i \mathrm{e}^{\lambda_i t_0} (\mathrm{e}^{-\lambda_i t_1} - \mathrm{e}^{-\lambda_i (t_1+\Delta_t)}) \end{aligned}, \tag{3.13}$$

where t_1 is the start of the next time interval. The expected weight is used to set the survival probability and the weight of surviving precursors, w_c'. If the expected delayed neutron weight is below the threshold weight limit W_{RR}, the Russian roulette is applied on the precursor, with survival probability

$$P_{surv} = \frac{w_{n,ex}}{W_{av}}. \tag{3.14}$$

If the precursor survives, it is stored for the next time interval with statistical weight

$$w_c' = w_c \frac{W_{av}}{w_{n,ex}}, \tag{3.15}$$

where W_{av} is the survival weight for neutrons (see Eq. (3.9)).

An alternative to the Russian roulette/splitting based population control in non-analog TDMC calculations is the combing method. The method normalizes the number of transported particles to the required number while preserving their total weight. Combing can be independently applied to both neutron and precursor populations. For the details of the method, the reader is referred to refs. [4, 62, 67].

3.2.4 Variance Reduction

Traditional variance reduction techniques used in steady-state Monte Carlo simulations, such as implicit capture, implicit fission, Russian roulette and splitting, can be applied in TDMC particle tracking as well. Methods implemented in the dynamic versions of Serpent and TRIPOLI-4 rely on such techniques [55, 62, 66].

Differently from static calculations, however, emission of multiple neutrons during a fission event causes branching in the simulation. This, in turn, causes fluctuation of the number of particles simulated during a time interval. Specifically, the chain starting from a single prompt neutron can be terminated after a single collision, or it can continue for many generations, producing many branches with secondary neutrons. The variance in neutron chain lengths causes variance in the results [4, 54, 68]. In contrast, during Monte Carlo criticality calculations the particles are simulated generation by generation and no chains are formed.

In an attempt to reduce the variance caused by branching, Sjenitzer and Hoogenboom [54] suggested using a branchless collision kernel. According to the method, a neutron entering a collision will either scatter or create a single new prompt fission neutron using implicit absorption. Hence, the branching process is changed into a single-branch process. In the case of scattering, the statistical weight of the neutron remains unchanged,

$$w_n' = w_n, \tag{3.16}$$

while the energy and the angle of the neutron are changed according to the scattering laws.

In the case of absorption, the weight of the neutron is adjusted as

$$w_n' = w_n \frac{\nu_p \Sigma_f + \Sigma_s}{\Sigma_t}, \tag{3.17}$$

where ν_p is the number of prompt neutrons and Σ_f, Σ_s, and Σ_t are the macroscopic fission, scattering and total cross-sections respectively. The new neutron energy is then sampled from the prompt neutron energy distribution and the new angle is sampled uniformly.

To ensure a fair game, the probability of scattering is modified as

$$P_s = \frac{\Sigma_s}{\nu_p \Sigma_f + \Sigma_s} \tag{3.18}$$

and the probability of absorption changed to

$$P_c = \frac{\nu_p \Sigma_f}{\nu_p \Sigma_f + \Sigma_s}, \tag{3.19}$$

so that $P_s + P_c = 1$.

The precursors are sampled in a conventional way. At every sampled collision, the precursors are generated with probability

$$P_p = w_n \frac{\nu_d \Sigma_f}{\Sigma_t}. \tag{3.20}$$

Treatment of delayed neutrons as discussed in Sec. 3.2.2 can be considered a variance reduction methodology as well since the sampling of delayed neutrons during each time interval is aimed at improving the statistics during the interval. According to Eq. (3.7), the weight of the emitted delayed neutron is proportional to the time interval length Δt. If the time intervals chosen for the simulation are small, the weights of the emitted delayed neutrons will be small as well. These neutrons may then be immediately killed by the Russian roulette, thus defeating the purpose of the forced precursor decay method [62].

To overcome this problem, Faucher et al. [62] introduced a time-dependent importance scheme. According to the scheme, a user-provided importance ratio between neutrons and precursors $R_i = I_{n,i}/I_{c,i}$ is used. Then, at the beginning of time interval i, the weights of neutrons, W_n, and precursors, W_c, are rescaled in such a way that the physical weights are preserved:

$$W'_{n,i+1} = W_{n,i+1} I_{n,i+1} = W_{n,i} I_{n,i}; \tag{3.21}$$

$$W'_{c,i+1} = W_{c,i+1} I_{c,i+1} = W_{c,i} I_{c,i}; \tag{3.22}$$

$$W'_{n,i+1} + W'_{c,i+1} = W_{n,i+1} + W_{c,i+1} = W_{n,i} + W_{c,i}. \tag{3.23}$$

The meaning of the importance factors $I_{n,i}$ and $I_{c,i}$ is that one particle (neutron or precursor respectively) represents $I_{n,i}$ and $I_{c,i}$ physical particles. The population weights are only adjusted if the importance ratio changes from time interval to time interval. Faucher et al. reported a figure-of-merit increase by a factor 63, for a 1 ms simulation of a critical system, using time intervals of 20 μs and a constant importance ratio of $R = 10^{-4}$ [62].

3.3 Transient Fission Matrix Method

Transient Fission Matrix (TFM) method was proposed as a computationally affordable approach to reactor kinetics and dynamics calculations, while retaining the flexibility of Monte Carlo methods [30, 69–73]. The fission matrix has been previously applied for solving various problems in stationary Monte Carlo reactor physics calculations [13, 17, 21, 25–28, 49]. The TFM method extends the use of the fission matrix to time-dependent problems; here, several variants of the fission matrix are pre-calculated using a stationary Monte Carlo solver and the database is then used to deterministically solve time-dependent problems. Because the fission matrices are sampled during Monte Carlo transport simulations, simplifications to

neutron transport and cross-section homogenization applied in traditional deterministic methods are avoided.

The TFM method was applied for calculating the kinetics and the kinetic parameters of Flattop and Jezebel experimental assemblies [30], dynamic 3D calculations of a Molten Salt Fast Reactor [72], and dynamic calculations of a Sodium Fast Reactor assembly [69–71, 73]. The authors of ref. [30] discuss two variants of the TFM method: "direct" and "fast" kinetics methods. The methods differ in the targeted accuracy and computing costs. The majority of the analyses reported in the literature were performed using the fast kinetics method [69–73]. Both variants of the TFM method are discussed further.

3.3.1 Direct TFM Method

For any given fission source distribution, the product of the fission matrix and the source vector would give the distribution of the next generation fission source,

$$\mathbf{S}_{g+1} = \mathbb{F} \cdot \mathbf{S}_g. \tag{3.24}$$

The authors of the TFM method [30] utilized this feature and included the time aspect by introducing a continuous operator $G_{\chi_p,\nu_p}(t', t, \mathbf{r}', \mathbf{r})$ associated to the time-dependent version of the fission matrix. This operator represents the probability that a prompt neutron created at t' in $\mathbf{r}'$ creates a new prompt neutron at t in $\mathbf{r}$. Subscripts χ_p and ν_p are used to denote the emission energy spectrum and the neutron production per fission used to calculate the operator. Since the multiplicities, ν, and the emission spectra, χ, are different for prompt and delayed neutrons, the authors considered four versions of the operator G: G_{χ_p,ν_p}, G_{χ_p,ν_d}, G_{χ_d,ν_p}, and G_{χ_d,ν_d}.

Because there is no interaction between the neutrons during transport (the transport equation is linear), the global response can be obtained by summing up the local responses. Hence, the prompt neutron source of generation $g+1$, $S_{g+1}(\mathbf{r}, t)$, can be calculated as the convolution of the operator G_{χ_p,ν_p} and the source of generation g, $S_g(\mathbf{r}', t')$ as [30]

$$\begin{aligned} &\left|G_{\chi_p,\nu_p}(t', t, \mathbf{r}', \mathbf{r})|S_g(\mathbf{r}', t')\right\rangle = \\ &\iint_{t'<t, \mathbf{r}' \in R} G_{\chi_p,\nu_p}(t', t, \mathbf{r}', \mathbf{r}) S_g(\mathbf{r}', t') \mathrm{d}\mathbf{r}' \mathrm{d}t' = S_{g+1}(\mathbf{r}, t), \end{aligned} \tag{3.25}$$

where the integration is carried out over all past times t' and space R. If the system is not changing between times t and t', G_{χ_p,ν_p} can be calculated for one initial time t' to all the subsequent times t, i.e. $G_{\chi_p,\nu_p}(t - t', \mathbf{r}', \mathbf{r})$.

Furthermore, the total prompt neutron source (in [neutrons/s]) at any time t can be expressed as the sum over all prompt source generations present at that time,

$$S(\mathbf{r}, t) = \sum_{g=1}^{\infty} S_g(\mathbf{r}, t). \tag{3.26}$$

Then, knowing the total prompt source at previous times t', the total prompt source at time t, $S(\mathbf{r},t)$, can be calculated as the convolution of G_{χ_p,ν_p} with the sum of the previous generations of source neutrons [30],

$$S(\mathbf{r},t) = |G_{\chi_p,\nu_p}(t-t',\mathbf{r}',\mathbf{r})|S(\mathbf{r}',t')\rangle. \tag{3.27}$$

The same argument can be made for delayed neutrons producing prompt neutrons, prompt neutrons producing precursors, and delayed neutrons producing precursors. Then, using operators for each process, G_{χ_p,ν_p}, G_{χ_p,ν_d}, G_{χ_d,ν_p}, and G_{χ_d,ν_d} the neutron kinetics can be expressed as [30]

$$\begin{aligned}\frac{dP_f(t,\mathbf{r})}{dt} = \frac{\beta_f}{\beta}\Big[&|G_{\chi_p,\nu_d}(t-t',\mathbf{r}',\mathbf{r})|S(\mathbf{r}',t')\rangle + \\ &|G_{\chi_d,\nu_d}(t-t',\mathbf{r}',\mathbf{r})|\sum_f \lambda_f P_f(t',\mathbf{r}')\rangle\Big] - \lambda_f P_f,\end{aligned} \tag{3.28}$$

$$S(t,\mathbf{r}) = |G_{\chi_p,\nu_p}(t-t',\mathbf{r}',\mathbf{r})|S(\mathbf{r}',t')\rangle + |G_{\chi_d,\nu_p}(t-t',\mathbf{r}',\mathbf{r})|\sum_f \lambda_f P_f(t',\mathbf{r}')\rangle. \tag{3.29}$$

Here $P_f(\mathbf{r},t)$ is used to denote the population of precursors in family f, position $\mathbf{r}$, and time t; $S(\mathbf{r},t)$ is the prompt neutron source production rate at position $\mathbf{r}$ and time t. The precursor production is split according to the family f using the normalized delayed neutron fraction β_f/β, where

$$\sum_f \frac{\beta_f}{\beta} = 1. \tag{3.30}$$

The operators in Eqs. (3.28)-(3.29) are then discretized in space and time, and are estimated during a Monte Carlo transport calculation. Let us denote the discretized operator by $\mathbb{G}(\Delta t_k)$, where Δt_k denotes the k^{th} time bin,

$$\mathbb{G}(\Delta t_k) = \begin{bmatrix} g_{1,1}(\Delta t_k) & g_{1,2}(\Delta t_k) & \cdots & g_{1,j}(\Delta t_k) \\ g_{2,1}(\Delta t_k) & g_{2,2}(\Delta t_k) & \cdots & g_{2,j}(\Delta t_k) \\ \vdots & \vdots & \ddots & \vdots \\ g_{i,1}(\Delta t_k) & g_{i,2}(\Delta t_k) & \cdots & g_{i,j}(\Delta t_k) \end{bmatrix}. \tag{3.31}$$

Here the indexes i and j are used to denote the volume cells.

The matrix element of the discretized operator, $g_{i,j}(\Delta t_k)$, represents the probability that a neutron created in cell j during bin time Δt_0 produces a neutron in cell i during bin time Δt_k. The element can be estimated as [30]

$$g_{i,j}(\Delta t_k) = \int_{t'\in\Delta t_0}\int_{\mathbf{r}'\in j}\int_{t\in\Delta t_k}\int_{\mathbf{r}\in i} G(t-t',\mathbf{r}',\mathbf{r})\frac{\mathrm{d}t'}{\Delta t_0}\frac{\mathrm{d}\mathbf{r}'}{V_j}\mathrm{d}t\,\mathrm{d}\mathbf{r}. \tag{3.32}$$

The fission neutron generation distribution in time, in cell i, due to a neutron born in cell j can then be reconstructed by selecting an appropriate time bin size and number to capture the shape of the pulse.

Laureau et al. [30] used the fixed-source calculations in MCNP to estimate the discretized operator and verified the approach by comparing the calculated and measured α-Rossi observables of Flattop and Jezebel critical assemblies. Agreement with measured data was reported within the error bounds. The kinetics of Flattop assembly were then calculated using Eq. (3.29) and benchmarked against a TDMC calculation using Serpent. The simulated time was 10 μs and the delayed neutrons were ignored. Both approaches were reported to agree within the statistical error. Time bin sizes of 0.025 ns were used to score the discretized operator $\mathbb{G}$. The authors concluded that significant computing effort is required for the direct calculation using Eqs. (3.28) and (3.29). Therefore a simplified, "fast", method was introduced. This method is discussed in the following section.

3.3.2 Fast TFM Method

Instead of treating the full time distribution of the response through operator $G(t-t', \mathbf{r}', \mathbf{r})$, the average response time from $\mathbf{r}'$ to $\mathbf{r}$ can be expressed through a separate time operator $T_{\chi_p,\nu_p}(\mathbf{r}', \mathbf{r})$, defined as [30]

$$T_{\chi_p,\nu_p}(\mathbf{r}', \mathbf{r}) = \frac{\int_{\tau>0} G_{\chi_p,\nu_p}(\tau, \mathbf{r}', \mathbf{r}) \cdot \tau \mathrm{d}\tau}{\int_{\tau>0} G_{\chi_p,\nu_p}(\tau, \mathbf{r}', \mathbf{r}) \mathrm{d}\tau}, \tag{3.33}$$

where $\tau = t - t'$. Hence, the operator T_{χ_p,ν_p} corresponds to the first moment of the time response. The space-discretized version of the operator will be denoted as $\mathbb{T}_{\chi_p,\nu_p}$.

In the simplified, fast TFM method, the time aspect is considered only through the time matrix $\mathbb{T}_{\chi_p,\nu_p}$. The time matrix contains the information of the average time response from cell j to cell i associated with the prompt neutron transport between the two cells. Stated differently, it describes the average time from a fission event in cell j to the fission event in cell i.

Because the response time is considered through operator T_{χ_p,ν_p}, the operators G_{χ_x,ν_x} are integrated over time,

$$\hat{G}_{\chi_x,\nu_x}(\mathbf{r}', \mathbf{r}) = \int t G_{\chi_x,\nu_x}(t - t', \mathbf{r}', \mathbf{r}) \mathrm{d}t', \tag{3.34}$$

and their discretized versions correspond to traditional fission matrices, which are scored for different neutron emission spectra (χ_p or χ_d) and multiplicities (ν_p or ν_d). These matrices will be denoted as $\mathbb{G}_{\chi_p,\nu_p}$, $\mathbb{G}_{\chi_p,\nu_d}$, $\mathbb{G}_{\chi_d,\nu_p}$ and $\mathbb{G}_{\chi_d,\nu_d}$. The authors of [69–73] scored the different versions of the fission matrices and the time matrix during Monte Carlo criticality calculations.

Further, it is assumeed that the time-dependent behaviour of prompt neutrons can be described by one effective fission-to-fission time l_{eff}, which is calculated from the time matrix $\mathbb{T}_{\chi_p,\nu_p}$ as [30, 72]

$$l_{eff} = \frac{\mathbf{N}_p^*(\mathbb{G}_{\chi_p,\nu_p} \cdot \mathbb{T}_{\chi_p,\nu_p})\mathbf{N}_p}{\mathbf{N}_p^* \mathbb{G}_{\chi_p,\nu_p} \mathbf{N}_p}, \tag{3.35}$$

where $(\mathbb{G}_{\chi_p,\nu_p} \cdot \mathbb{T}_{\chi_p,\nu_p})$ denotes the matrix element-to-element multiplication, which gives the neutron production associated to the response time from j to i, $\mathbf{N}_p$ is the eigenvector of $\mathbb{G}_{\chi_p,\nu_p}$, and $\mathbf{N}_p^*$ is the eigenvector of the transposed fission matrix $\mathbb{G}^T_{\chi_p,\nu_p}$. The transposed matrix describes the backward transport of neutrons, so the eigenvector $\mathbf{N}_p^*$ gives the importance map. Therefore, l_{eff} can be interpreted as the adjoint-weighted response time between the successive prompt neutron generations.

Next, first-order balance equations are formulated for the neutron vector $\mathbf{N}$ and precursor vectors $\mathbf{P}_f$ [30, 72],

$$\frac{\mathrm{d}\mathbf{N}(t)}{\mathrm{d}t} = \mathbb{G}_{\chi_p,\nu_p}\mathbf{N}(t)\frac{1}{l_{eff}} + \mathbb{G}_{\chi_d,\nu_p}\sum_f \lambda_f \mathbf{P}_f(t) - \frac{1}{l_{eff}}\mathbf{N}(t), \tag{3.36}$$

$$\frac{\mathrm{d}\mathbf{P}_f(t)}{\mathrm{d}t} = \frac{\beta_f}{\beta}\left[\mathbb{G}_{\chi_p,\nu_d}\mathbf{N}(t)\frac{1}{l_{eff}} + \mathbb{G}_{\chi_d,\nu_d}\sum_f \lambda_f \mathbf{P}_f(t)\right] - \lambda_f \mathbf{P}_f(t), \tag{3.37}$$

where f is used to denote the precursor family. Equations (3.36)-(3.37) describe the neutron balance through production due to prompt neutron-induced fissions (first term), delayed neutron-induced fissions (second term), and prompt neutron removal (third term). The precursor balance is expressed through production due to prompt neutron-induced fissions (first term), delayed neutron-induced fissions (second term), and precursor decay (third term). Here it is assumed that the delayed neutron transport time is negligible compared to the precursor decay time.

3.4 Time-Dependent Response Matrix Methods

While a significant amount of literature is available on stationary response matrix methods [31, 32, 34–45], the time-dependent response matrix methods appear to be less mature. Only several publications on aspects of time dependence are available in the literature [74–78]. Recent publications deal with the fundamentals of time dependence and solve several simplified problems. Pounders and Rahnema [76] derived the response equations for a semi-infinite fissile slab, based on the Legendre series expansion of the time variable. In a later publication [77], the whole phase-space dependence was addressed. Delayed neutrons were not considered in both publications. Roberts [78] then showed the equivalence between the latter method and the methods published more than forty years ago [74, 75], generalized the time-dependent method to arbitrary expansions and expansion orders, included delayed neutrons, and demonstrated the approach on several infinite homogeneous medium problems.

The time-dependent response matrix formalism can be understood through applying the Green's function to the transport problem (Eq. (3.1)), defined over a node V_i of a space-discretized system. When the global volume is decomposed into a three-dimensional Cartesian mesh, then each node V_i is bounded by six surfaces

∂V_{i_k} and the local transport problem can be defined as

$$\begin{aligned}\frac{1}{v}\frac{\partial\psi(\mathbf{r},\mathbf{\Omega},E,t)}{\partial t} + \mathbf{M}\psi(\mathbf{r},\mathbf{\Omega},E,t) &= s(\mathbf{r}_n,\mathbf{\Omega},E,t)\\ &+ \sum_{k=1}^{6}\hat{\mathbf{n}}_{i_k}\cdot\mathbf{j}_G(\mathbf{r},\mathbf{\Omega},E,t)H(-\mathbf{\Omega}\cdot\hat{\mathbf{n}}_{i_k})\delta(\mathbf{r}-\mathbf{r}_k)\\ &+ \frac{1}{v}\psi_G(\mathbf{r},\mathbf{\Omega},E,0)\delta(t) \quad \text{with } \mathbf{r}\in V_i, \text{ and } \mathbf{r}_k\in\partial V_{i_k},\end{aligned} \tag{3.38}$$

where $\hat{\mathbf{n}}_{i_k}$ is the outward normal of ∂V_{i_k}, H is the Heaviside step function, δ is the Dirac's δ-function, and the loss operator $\mathbf{M}$ (see Sec. 2.3) was introduced to simplify the notation. The source terms on the right-hand side consist of the volumetric source (first term) which includes contributions from fission, decay of delayed neutron precursors, and external sources (if any); boundary conditions on the six node surfaces (second term) which are driven by the global angular current $\mathbf{j}_G = \mathbf{\Omega}\psi_G$; and the global initial condition (third term).

By defining the Green's function G to the local problem, like that given by Eq. (3.38), the solution can be expressed for any arbitrary source $S(\mathbf{r},\mathbf{\Omega},E,t)$ as

$$\begin{aligned}\psi(\mathbf{r},\mathbf{\Omega},E,t) = \int_{\mathbf{r}'\in V_i}\mathrm{d}\mathbf{r}'\int_{4\pi}\mathrm{d}\mathbf{\Omega}'\int_0^\infty\mathrm{d}E'\int_{-\infty}^{t}\mathrm{d}t' S(\mathbf{r}',\mathbf{\Omega}',E',t')\times\\ G(\mathbf{r}',\mathbf{\Omega}',E',t'\to\mathbf{r},\mathbf{\Omega},E,t).\end{aligned} \tag{3.39}$$

Consequently, the solution of Eq. (3.38) can be decomposed according to the three source terms on the right-hand side,

$$\psi(\mathbf{r},\mathbf{\Omega},E,t) = \psi_s(\mathbf{r},\mathbf{\Omega},E,t) + \sum_{k=1}^{6}\psi_{c_k}(\mathbf{r},\mathbf{\Omega},E,t) + \psi_0(\mathbf{r},\mathbf{\Omega},E,t), \tag{3.40}$$

where ψ_s, ψ_{c_k}, and ψ_0 are contributions from volume sources, incident currents and initial values respectively. Each of the contributions can be expressed by convoluting the Green's function with the respective source term, as in Eq. (3.39). Hence, the time-dependent response equations would consist of a sum of convolution integrals for various surface or volumetric sources with the respective time-dependent response kernels defined through the Green's function.

The equations for outgoing partial currents on each node surface can be defined directly from the angular flux, e.g. for surface k as

$$j^+_{i_k}(\mathbf{r},\mathbf{\Omega},E,t) = \hat{\mathbf{n}}_{i_k}\cdot\mathbf{\Omega}\big(\psi_s(\mathbf{r},\mathbf{\Omega},E,t) + \sum_{k=1}^{6}\psi_{c_k}(\mathbf{r},\mathbf{\Omega},E,t) + \psi_0(\mathbf{r},\mathbf{\Omega},E,t)\big). \tag{3.41}$$

The partial currents are then used to couple the local solutions using the connectivity matrix, obtaining the global solution.

Let us further consider the time variable only (other phase-space variables were discussed in Section 2.5.2) and limit the discussion to partial currents $j^{\pm 1}$. The

[1] Details regarding prompt and delayed volumetric sources are provided in Paper II

generalized time-dependent response equation is then given by [75]

$$j^+(t) = \int_{-\infty}^{t} R(t' \to t) j^-(t') \mathrm{d}t'. \tag{3.42}$$

Here the kernel $R(t' \to t)$ gives the outgoing partial currents at time t due to a burst of incoming partial currents at time t'. The analysis is further limited to $t \in (0, \infty)$ by introducing initial conditions [75–78], and assuming that the system does not vary with time within some considered time interval τ, so that the kernels become functions of $\tau = t - t'$. The integrals, like in Eq. (3.42) are then commonly treated by looking for a basis to expand the time variable combined with other phase-space expansions as discussed in Section 2.5.2.

By expanding the time variable on a Legendre polynomial basis [76,77], or basis consisting of exponential functions [78], the authors show that Eqs. (3.40) and (3.41) can be reduced to a linear system for the nodal flux and current moments, where the moments of ψ and $j^{\pm}$ are expressed as vectors and the nodal response function moments are expressed as matrices. Computing the moments from the linear system gives the solution after a time interval τ, over which the time expansion has been integrated. This solution is then used as the initial condition to calculate the solution after the next time interval.

The response kernel in Eq. (3.42) consists of multiple components with significantly different time constants. Sicilian [74] and Pryor [75] explained, that the fast component results from prompt events, such as the transmission of un-collided neutrons, the transmission of scattered neutrons, and escape of prompt fission neutrons, while the slow component results from the escape of delayed neutrons. If the emission of the delayed neutrons is implicitly included in the response kernels, the selected basis functions have to be adequate for capturing the different time scales [78].

Alternatively, Pryor [75] suggested to treat the delayed neutron precursors explicitly. Then, the prompt, R_p, and delayed, R_d, responses can be split into two integrals as

$$j^+(t) = \int_{-\infty}^{t} R_p(t' \to t) j^+(t') \mathrm{d}t' + \int_{-\infty}^{t} R_d(t' \to t) \sum_i \lambda_i C_i(t') \mathrm{d}t'. \tag{3.43}$$

Note that in this definition the prompt volumetric source is implicitly included in the current response. The kernels R_p and R_d, now have only the fast component, since the time delay of the delayed neutron emission is explicitly governed by the precursor concentration equation, which for group i the author expressed as

$$\frac{\mathrm{d}C_i}{\mathrm{d}t} = -\lambda_i C_i + \beta_i \nu \Sigma_f \phi(t). \tag{3.44}$$

More generally, the precursor concentration can be defined by considering the response form of Eq. (3.2).

Similarly to the approach by Prior [75], in Paper II we define the response functions by explicitly considering the prompt and delayed volumetric sources in addition to the partial currents. Hence, we obtain three response equations for the prompt source, the delayed neutron precursor concentration, and the partial currents. Using such definition the response time-scale becomes of the order of a neutron lifetime, so we use a simple linear dependence to treat the time variable. We further eliminate the non-temporal phase-space dependence by weighing the response kernels on the critical solution. This leads to a method similar to the fast TFM method discussed in Section 3.3; the response kernels can be estimated during a set of Monte Carlo criticality simulations and then used to solve the space-time dependent problem. However, instead of considering a single, space-discretized Green's function for the entire system, i.e. the fission matrix, the Green's functions in the response equations, i.e. the response kernels, are defined for each source term and each node of the discretized system. This way the neutron transport in a node depends only on the information from the neighbouring nodes as compared to the fission matrix, where each node is coupled with all other nodes in the system.

Chapter 4

Summary of the Included Papers

4.1 Paper I

Paper I proposes a neutron population size control method for Monte Carlo criticality calculations. The method gradually increases the neutron population size during subsequent criticality cycles. This improves the efficiency of criticality calculations, as the source can be rapidly (in terms of CPU time) iterated at the beginning of the calculations using small population size, and as the population size gradually increases, the fission source bias is prevented from dominating the total error throughout the calculation. The paper proposes a simple analytical expression for determining the optimal population size, based on the number of neutron histories simulated previously. The proposed method was tested on a set of full-core PWR calculations, where a higher figure-of-merit was observed compared to conventional Monte Carlo criticality calculations using a fixed neutron population size.

4.2 Paper II

Paper II proposes a stochastic-deterministic time-dependent response matrix method. The method uses sets of response functions which are pre-computed during Monte Carlo criticality calculations corresponding to the various states of the analysed system. The response functions are then used in a set of deterministic equations describing the space-time evolution of the system. This constitutes a novel approach to using the information from Monte Carlo criticality calculations for solving space-time dependent problems. The paper includes an exhaustive description of the method and provides two demonstrations of kinetic transients in a 3×3 assembly PWR mini-core. The time-evolution of the system power obtained with the proposed method was compared to time-dependent Monte Carlo calculations. A qualitative agreement was observed between the two methods, while it was indicated that a rigorous benchmarking should be performed after implementing the method in an established Monte Carlo code.

Chapter 5

Conclusions and Outlook

This thesis focused on criticality and time-dependent problems in reactor physics. Monte Carlo methods proposed for solving such problems more efficiently were overviewed. The included papers address the efficiency issue as well. The first paper proposes a method aimed at running efficient Monte Carlo criticality calculations through control of neutron population size. The second paper proposes a new approach for using the response matrix formalism in time-dependent reactor physics problems. The proposed methods were tested on several example problems giving promising results, nevertheless, further investigation is necessary to assess the full potential of the methods.

The population control method may be tested using a number of representative geometries, comparing the method with other proposed approaches. Furthermore, the method may be applied in problems where data from Monte Carlo criticality calculations are used for coupled solutions, e.g. in Monte Carlo burn-up problems.

The time-dependent response matrix method needs to be better understood as well. First, insight into how the selection of node size and the statistical error in the scored responses affect the time-dependent solution is necessary. In addition, other challenges can be foreseen, such as response parametrization with respect to state variables, necessary for dynamic problems. To address these questions, implementation of the time-dependent response matrix method into a robust Monte Carlo reactor physics code is needed, which would allow for rigorous benchmarking against other methods thus facilitating the analyses.

Bibliography

[1] V. Masson-Delmotte, P. Zhai, H.-O. Pörtner, D. Roberts, J. Skea, P. Shukla, A. Pirani, W. Moufouma-Okia, C. Péan, R. Pidcock, S. Connors, J. Matthews, Y. Chen, X. Zhou, M. Gomis, E. Lonnoy, T. Maycock, M. Tignor, and T. Waterfield, "Global Warming of 1.5°C. An IPCC Special Report on the impacts of global warming of 1.5°C above pre-industrial levels and related global greenhouse gas emission pathways, in the context of strengthening the global response to the threat of climate change," tech. rep., IPCC, 2018.

[2] G. I. Bell and S. Glasstone, *Nuclear Reactor Theory*. Van Nostrand Reinhold Company, 1970.

[3] J. J. Duderstadt and L. J. Hamilton, *Nuclear Reactor Analysis*. John Wiley & Sons, Inc., 1976.

[4] B. L. Sjenitzer, *The Dynamic Monte Carlo Method for Transient Analysis of Nuclear Reactors*. Phd thesis, Technische Universiteit Delft, 2013.

[5] J. Leppänen, M. Pusa, T. Viitanen, V. Valtavirta, and T. Kaltiaisenaho, "The Serpent Monte Carlo code: Status, development and applications in 2013," *Annals of Nuclear Energy*, vol. 82, pp. 142–150, 2015.

[6] J. E. Hoogenboom, W. R. Martin, and B. Petrovic, "Monte carlo performance benchmark for detailed power density calculation in a full size reactor core benchmark specifications," 2010.

[7] T. E. Booth, "Common misconceptions in Monte Carlo particle transport," *Applied Radiation and Isotopes*, vol. 70, no. 7, pp. 1042–1051, 2012.

[8] X-5 Monte Carlo Team, "MCNP - a general monte carlo N-particle transport code, version 5. volume i: Overview and theory," Tech. Rep. LA-UR-03-1987, Los Alamos National Lab. (LANL), 2005.

[9] J. Leppänen, T. Kaltiaisenaho, V. Valtavirta, and M. Metsälä, "Development of a Coupled Neutron / Photon Transport Mode in the Serpent 2 Monte Carlo Code," in *M&C 2017 - International Conference on Mathematics & Computational Methods Applied to Nuclear Science & Engineering*, (Jeju, Korea), 2017.

[10] J. Leppänen, *Development of a new Monte Carlo reactor physics code.* PhD thesis, VTT Technical Research Centre of Finland, 2007.

[11] C. J. Josey, "General improvements to the MCNP alpha-eigenvalue solver," Tech. Rep. LA-UR-18-22738, Los Alamos National Lab. (LANL), 2018.

[12] D. E. Cullen, C. J. Clouse, R. Procassini, and R. C. Little, "Static and dynamic criticality: Are they different?," Tech. Rep. UCRL-TR-201506, Lawrence Livermore National Lab., 2003.

[13] S. Carney, F. Brown, B. Kiedrowski, and W. Martin, "Theory and applications of the fission matrix method for continuous-energy Monte Carlo," *Annals of Nuclear Energy*, vol. 73, pp. 423–431, 2014.

[14] F. B. Brown, S. E. Carney, B. C. Kiedrowski, and W. R. Martin, "Fission Matrix Capability for MCNP, Part I - Theory," in *International Conference on Mathematics and Computational Methods Applied to Nuclear Science & Engineering (M&C 2013)*, (Sun Valley, Idaho, USA), p. 12, American Nuclear Society, LaGrange Park, IL, 2013.

[15] A. Haghighat, *Monte Carlo Methods for Particle Transport.* CRC Press, 2014.

[16] J. D. Hoffman, *Numerical Methods for Engineers and Scientists.* CRC Press, 2001.

[17] K. Tuttelberg, *STORM in Monte Carlo reactor physics calculations.* Msc thesis, KTH Royal Institute of Technology, 2014.

[18] K. Tuttelberg and J. Dufek, "Estimation of errors in the cumulative Monte Carlo fission source," *Annals of Nuclear Energy*, vol. 72, pp. 151–155, 2014.

[19] T. Ueki, F. B. Brown, D. K. Parsons, and D. E. Kornreich, "Autocorrelation and dominance ratio in monte carlo criticality calculations," *Nuclear Science and Engineering*, vol. 145, 11 2003.

[20] R. J. Brissenden and A. R. Garlick, "BIASES IN THE ESTIMATION OF Keff AND ITS ERROR BY MONTE CARLO METHODS," *Annals of Nuclear Energy*, vol. 13, no. 2, pp. 63–83, 1986.

[21] J. Dufek, *Development of New Monte Carlo Methods in Reactor Physics.* Phd thesis, School of Engineering Sciences, KTH Royal Institute of Technology, 2009.

[22] T. Yamamoto and Y. Miyoshi, "Reliable Method for Fission Source Convergence of Monte Carlo Criticality Calculation with Wielandt's Method," *Journal of Nuclear Science and Technology*, vol. 41, no. 2, pp. 99–107, 2004.

[23] M. J. Lee, H. G. Joo, D. Lee, and K. Smith, "Coarse mesh finite difference formulation for accelerated Monte Carlo eigenvalue calculation," *Annals of Nuclear Energy*, vol. 65, pp. 101–113, 2014.

[24] T. Kitada and T. Takeda, "Effective Convergence of Fission Source Distribution in Monte Carlo Simulation," *Journal of Nuclear Science and Technology*, vol. 38, no. 5, pp. 324–329, 2001.

[25] J. Dufek and W. Gudowski, "Stability and convergence problems of the Monte Carlo fission matrix acceleration methods," *Annals of Nuclear Energy*, vol. 36, no. 10, pp. 1648–1651, 2009.

[26] J. Dufek and G. Holst, "Correlation of errors in the Monte Carlo fission source and the fission matrix fundamental-mode eigenvector," *Annals of Nuclear Energy*, vol. 94, pp. 415–421, 2016.

[27] J. Dufek and W. Gudowski, "Fission matrix based Monte Carlo criticality calculations," *Annals of Nuclear Energy*, vol. 36, no. 8, pp. 1270–1275, 2009.

[28] J. Dufek and W. Gudowski, "An efficient parallel computing scheme for Monte Carlo criticality calculations," *Annals of Nuclear Energy*, vol. 36, no. 8, pp. 1276–1279, 2009.

[29] W. J. Walters, N. J. Roskoff, and A. Haghighat, "The rapid fission matrix approach to reactor core criticality calculations," *Nuclear Science and Engineering*, vol. 192, no. 1, pp. 21–39, 2018.

[30] A. Laureau, M. Aufiero, P. R. Rubiolo, E. Merle-Lucotte, and D. Heuer, "Transient Fission Matrix: Kinetic calculation and kinetic parameters βeff and Λeff calculation," *Annals of Nuclear Energy*, vol. 85, pp. 1035–1044, 2015.

[31] Z. Weiss and S.-Ö. Lindahl, "High-Order Response Matrix Equations in Two-Dimensional Geometry," *Nuclear Science and Engineering*, vol. 58, no. 2, pp. 166–181, 1975.

[32] S.-Ö. Lindahl and Z. Weiss, "The Response Matrix Method," in *Advances in Nuclear Science and Technology* (J. Lewins, ed.), pp. 73–154, New York: Springer, 1981.

[33] Y. Azmy and E. Sartori, *Nuclear Computational Science: A Century in Review*. Springer, 2010.

[34] K. J. Connolly, F. Rahnema, and D. Zhang, "A coarse mesh radiation transport method for 2-D hexagonal geometry," *Annals of Nuclear Energy*, vol. 42, pp. 1–10, 2012.

[35] D. Zhang and F. Rahnema, "An efficient hybrid stochastic/deterministic coarse mesh neutron transport method," *Annals of Nuclear Energy*, vol. 41, pp. 1–11, 2012.

[36] J. A. Roberts, *Advanced Response Matrix Methods for Full Core Analysis*. Phd thesis, Massachusetts Institute of Technology, 2014.

[37] J. A. Roberts and B. Forget, "Solving eigenvalue response matrix equations with nonlinear techniques," *Annals of Nuclear Energy*, vol. 69, pp. 97–107, 2014.

[38] M. Moriwaki, K. Ishii, H. Maruyama, and M. Aoyama, "A new direct calculation method of response matrices using a monte carlo calculation," *Journal of Nuclear Science and Technology*, vol. 36, no. 10, pp. 877–887, 1999.

[39] B. Forget, *A Three Dimensional Heterogeneous Coarse Mesh Transport Method for Reactor Calculations*. Phd thesis, Georgia Institute of Technology, 2006.

[40] K. ISHII, T. HINO, T. MITSUYASU, and M. AOYAMA, "Three-Dimensional Direct Response Matrix Method Using a Monte Carlo Calculation," *Journal of Nuclear Science and Technology*, vol. 46, no. 3, pp. 259–267, 2009.

[41] T. Mitsuyasu, K. Ishii, T. Hino, and M. Aoyama, "Development of Spectral History Methods for Pin-By-Pin Core Analysis Method Using Three-Dimensional Direct," *Journal of Nuclear Science and Technology*, vol. 47, no. 12, pp. 1124–1130, 2009.

[42] T. Hino, K. Ishii, T. Mitsuyasu, and M. Aoyama, "BWR Core Simulator Using Three-Dimensional Direct Response Matrix and Analysis of Cold Critical Experiments," *Journal of Nuclear Science and Technology*, vol. 47, no. 5, pp. 482–491, 2010.

[43] J. Leppänen, T. Viitanen, and O. Hyvönen, "Development of a Variance Reduction Scheme in the Serpent 2 Monte Carlo Code," in *M&C 2017 - International Conference on Mathematics & Computational Methods Applied to Nuclear Science & Engineering*, (Jeju, Korea), 2017.

[44] F. Rahnema and D. Zhang, "Continuous energy coarse mesh transport (COMET) method," *Annals of Nuclear Energy*, vol. 115, pp. 601–610, 2018.

[45] J. Leppänen, "Acceleration of fission source convergence in the serpent 2 monte carlo code using a response matrix based solution for the initial source distribution," in *PHYSOR 2018: Reactor Physics paving the way towards more efficient systems*, (Cancun, Mexico), 2018.

[46] J. Leppänen, "Acceleration of fission source convergence in the Serpent 2 Monte Carlo code using a response matrix based solution for the initial source distribution," *Annals of Nuclear Energy*, vol. 128, pp. 63–68, 2019.

[47] F. B. Brown, W. R. Martin, J. Leppanen, W. Haeck, and B. Cochet, "Reactor Physics Analysis with Monte Carlo," Tech. Rep. LA-UR-10-02762, Los Alamos National Lab. (LANL), 2010.

[48] K. Tuttelberg and J. Dufek, "Neutron batch size optimisation methodology for Monte Carlo criticality calculations," *Annals of Nuclear Energy*, vol. 75, pp. 620–626, 2015.

[49] J. Dufek and K. Tuttelberg, "Monte Carlo criticality calculations accelerated by a growing neutron population," *Annals of Nuclear Energy*, vol. 94, no. March, pp. 16–21, 2016.

[50] E. L. Kaplan, "Monte carlo methods for equilibrium solutions in neutron multiplication," Tech. Rep. UCRL-5275T, Lawrence Livermore Laboratory, 1958.

[51] A. Zhitnik, N. Ivanov, V. Marshalkin, S. Ognev, A. Pevnitsky, V. Povyshev, I. Ponomarev, V. Roslov, T. Semenova, V. Tarasov, V. Fomin, T. Taiwo, and W. Yang, "Code TDMCC for Monte Carlo computations of spatial reactor core kinetics," in *The Monte Carlo Method: Versatility Unbounded In A Dynamic Computing World*, (Chattanooga, Tennessee), pp. 1–12, American Nuclear Society, LaGrange Park, IL, 2005.

[52] E. V. Artemeva, V. V. Bakanov, E. N. Donskoy, A. K. Zhitnik, N. V. Ivanov, S. P. Ognev, A. B. Ronzhin, V. I. Roslov, and T. V. Semenova, "Monte Carlo Simulation of Joint Transport of Neutrons and Photons," in *Proceedings of 5LC*, pp. 1–10, 2005.

[53] B. L. Sjenitzer and J. E. Hoogenboom, "A Monte Carlo Method for Calculation of the Dynamic Behaviour of Nuclear Reactors," *Progress in NUCLEAR SCIENCE and TECHNOLOGY*, vol. 2, no. October, pp. 716–721, 2011.

[54] B. Sjenitzer and E. Hoogenboom, "Dynamic Monte Carlo Method for Nuclear Reactor Kinetics Calculations," *Nuclear Science and Engineering*, vol. 175, no. 1, pp. 94–107, 2013.

[55] J. Leppänen, "Development of a dynamic simulation mode in serpent 2 Monte Carlo code," in *International Conference on Mathematics and Computational Methods Applied to Nuclear Science and Engineering (M&C 2013)*, (Sun Valley, Idaho), pp. 117–127, 2013.

[56] L. F. Russell, *Simulation of Time-Dependent Neutron Populations for Reactor Physics Applications Using the Geant4 Monte Carlo Toolkit.* Msc thesis, McMaster University, Hamilton, Ontario, Canada, 2012.

[57] L. Russell, A. Buijs, and G. Jonkmans, "G4-STORK: A Geant4-based Monte Carlo reactor kinetics simulation code," *Annals of Nuclear Energy*, vol. 71, pp. 451–461, 2014.

[58] N. Shaukat, M. Ryu, and H. J. Shim, "Dynamic Monte Carlo transient analysis for the OECD/NEA C5G7-TD benchmark," *Nuclear Engineering and Technology*, vol. 49, no. June, pp. 1–8, 2017.

[59] N. Shaukat, M. Ryu, and H. J. Shim, "Dynamic Monte Carlo transient analysis for the Organization for Economic Co-operation and Development Nuclear Energy Agency (OECD/NEA) C5G7-TD benchmark," *Nuclear Engineering and Technology*, vol. 49, pp. 920–927, 2017.

[60] A. G. Mylonakis, M. Varvayanni, D. G. Grigoriadis, and N. Catsaros, "Developing and investigating a pure Monte-Carlo module for transient neutron transport analysis," *Annals of Nuclear Energy*, vol. 104, pp. 103–112, 2017.

[61] A. Srivastava, K. P. Singh, and S. B. Degweker, "Monte Carlo Methods for Reactor Kinetic Simulations," *Nuclear Science and Engineering*, vol. 189, no. 2, pp. 152–170, 2017.

[62] M. Faucher, D. Mancusi, and A. Zoia, "New kinetic simulation capabilities for TRIPOLI-4®: Methods and applications," *Annals of Nuclear Energy*, vol. 120, pp. 74–88, 2018.

[63] B. L. Sjenitzer, J. E. Hoogenboom, J. Jiménez Escalante, and V. Sanchez Espinoza, "Coupling of dynamic Monte Carlo with thermal-hydraulic feedback," *Annals of Nuclear Energy*, vol. 76, pp. 27–39, 2015.

[64] A. Levinsky, V. Valtavirta, F. P. Adams, V. N. P. Anghel, and T.-d. M. Carlo, "Annals of Nuclear Energy Modeling of the SPERT transients using Serpent 2 with time-dependent capabilities," *Annals of Nuclear Energy*, vol. 125, pp. 80–98, 2019.

[65] J. Dorning, "Nuclear reactor kinetics: 1934-1999 and beyond," in *Nuclear Computational Science: A Century in Review* (Y. Azmy and E. Sartori, eds.), ch. 8, pp. 375–457, Springer, 2010.

[66] V. Valtavirta, M. Hessan, and J. Leppänen, "Delayed neutron emission model for time dependent simulations with the serpent 2 monte carlo code," in *PHYSOR 2016*, (Sun Valley, Idaho), 2016.

[67] T. E. Booth, "A WEIGHT (CHARGE) CONSERVING IMPORTANCE-WEIGHTED COMB FOR MONTE CARLO," in *Radiation Protection & Shielding Topical Meeting*, (No. Falmouth, Massachusetts), 1996.

[68] B. L. Sjenitzer and J. E. Hoogenboom, "General purpose dynamic Monte Carlo with continuous energy for transient analysis," in *PHYSOR 2012 Advances in Reactor Physics Linking Research, Industry, and Education*, (Knoxville, Tennessee, USA), 2012.

[69] A. Laureau, L. Buiron, B. Fontaine, and V. Pascal, "Fission Matrix Interpolation for the TFM Approach Based on a Local Correlated Sampling Technique for Fast Spectrum Heterogeneous Reactors," in *M&C 2017 - International Conference on Mathematics & Computational Methods Applied to Nuclear Science & Engineering*, (Jeju, Korea), 2017.

[70] A. Laureau, L. Buiron, and B. Fontaine, "Towards spatial kinetics in a low void effect sodium fast reactor: core analysis and validation of the TFM neutronic approach," *EPJ Nuclear Sciences & Technologies*, vol. 3, p. 17, 2017.

[71] A. Laureau, L. Buiron, and B. Fontaine, "Local correlated sampling Monte Carlo calculations in the TFM neutronics approach for spatial and point kinetics applications," *EPJ Nuclear Sciences & Technologies*, vol. 3, no. 16, 2017.

[72] A. Laureau, D. Heuer, E. Merle-Lucotte, P. R. Rubiolo, M. Allibert, and M. Aufiero, "Transient coupled calculations of the Molten Salt Fast Reactor using the Transient Fission Matrix approach," *Nuclear Engineering and Design*, vol. 316, pp. 112–124, 2017.

[73] A. Laureau, Y. Lederer, A. Krakovich, L. Buiron, and B. Fontaine, "Spatial analysis of unprotected transients in heterogeneous sodium fast reactors," *Annals of Nuclear Energy*, vol. 115, pp. 554–564, 2018.

[74] J. M. Sicilian, "Response Matrices in Space-Time Reactor Dynamics," *Nuclear Science and Engineering*, vol. 56, no. 3, pp. 291–300, 1975.

[75] R. Pryor, "Recent Developments in the Response Matrix Method," in *Advanced Reactors: Physics, Design and Economics* (J. Kallfelz and R. Karam, eds.), pp. 169–181, New York: Pergamon Press, 1975.

[76] J. M. Pounders and F. Rahnema, "A response-based time-dependent neutron transport method," *Annals of Nuclear Energy*, vol. 37, no. 11, pp. 1595–1600, 2010.

[77] J. Pounders and F. Rahnema, "A Coarse-Mesh Method for the Time-Dependent Transport Equation," *Nuclear Science and Engineering*, vol. 5639, pp. 273–291, 2014.

[78] J. A. Roberts, "A High-Order, Time-Dependent Response Matrix Method for Reactor Kinetics," *Nuclear Science and Engineering*, vol. 179, no. 3, pp. 333–341, 2015.